Labeled Random Finite Sets With Moment Approximation

Zhejun Lu, Weidong Hu, and Thia Kirubarajan

***Abstract*—The probability hypothesis density (PHD) filter was proposed as a practical approximation of the multitarget Bayes filter. The cardinalized PHD (CPHD) filter improves on the PHD filter by propagating cardinality distribution. However, both the PHD and CPHD filters have limitations in dealing with missed detections, extracting target state in their particle implementations, and maintaining track continuity. In this paper, based on the labeled random finite set theory, τ-labeled PHD and CPHD (τ-LPHD/LCPHD) filtering approaches, in which the PHD components are separated and uniquely identified by a tag τ, are proposed. Based on the information from the τ-LPHD/LCPHD filtering processes, new δ-generalized labeled PHD and CPHD filtering approaches are proposed to address the issues in the τ-LPHD/LCPHD filters, which are similar to the issues in the standard PHD/CPHD filters. The two proposed methods interact with each other and inherit the advantages of the δ-generalized labeled multi-Bernoulli filter, with substantial savings in computation resources.**

***Index Terms*—Multitarget tracking, finite set statistic, PHD, CPHD, GLMB.**

I. Introduction

In MULTITARGET tracking, the objective is to jointly estimate the number of targets and their states from a sequence of measurements. The challenges in achieving this objective include detection uncertainty, association uncertainty, and interference from false alarms (clutter) [1]–[3]. Conventional multitarget tracking filters typically associate measurements to tracks and then use a single target filter to estimate target state. The Kalman filter (KF) and Extended Kalman filter (EKF) are usually applied as the single target filter for linear and non-linear systems, respectively [4]. Many measurement-to-track association techniques have been proposed in the literature; the two most commonly used are the Multiple Hypothesis Tracking (MHT) algorithm [5] and Joint Probabilistic Data Association (JPDA) filter [6]. Since conventional multitarget filters track each target separately, there can be significant performance degradation when there is a large number of closely-spaced targets. Furthermore, they may yield unstable results when the number of targets is unknown and difficult to estimate [7].

Based on the Random Finite Set (RFS) theory, Finite Set Statistics (FISST) approach [3] provides a new systematic formulation for multitarget tracking called the multitarget Bayes filter. Due to the computational complexity of the optimal multitarget Bayes filter, several alternatives — including the Probability Hypothesis Density (PHD) filter [8], the Cardinalized PHD (CPHD) filter [9], the Multitarget Multi-Bernoulli (MeMBer) filter [3], and the Cardinality Balanced MeMBer (CBMeMBer) filter [10] — have been proposed as computationally tractable approximations. Based on moment approximation, the PHD filter propagates only the first moment of the multitarget density, while the CPHD filter also propagates the cardinality distribution. The MeMBer and CBMeMBer filters propagate the parameters of a multi-Bernoulli distribution to approximate the posterior multitarget density.

However, without explicit data association, these filters do not have the advantage of track continuity. Thus, it is not possible to determine which present-time track evolved from which previous track. Many methods have been proposed to maintain this track continuity problem. These methods are usually combined with the Sequential Monte Carlo (SMC) or Gaussian Mixture (GM) implementations, e.g., labeled particles [11] or Gaussian components [12], [13], or are combined with other traditional data association techniques [14]–[16].

The most theoretically rigorous and tractable approach is the recently proposed Generalized Labeled Multi-Bernoulli (GLMB) filter [17], [18], and its computationally efficient approximation, the Labeled Multi-Bernoulli (LMB) filter [19], which is based on the labeled RFS theory. The labeled RFS outputs target trajectories and distinguishes them by unique labels; thus, the trajectory estimates can be obtained without other post-processing. Moreover, the GLMB is a conjugate prior, which is closed under the Chapman-Kolmogorov equation with the standard multi-object likelihood [17].

Among the multitarget Bayes filters, the PHD and CPHD filters are the most efficient to implement because of their elegant formulation and tractable computational complexity. But, the cardinality estimate in the PHD filter is often unstable due to the

Manuscript received May 11, 2016; revised October 12, 2016 and January 8, 2017; accepted March 12, 2017. Date of publication March 29, 2017; date of current version April 27, 2017. The associate editor coordinating the review of this manuscript and approving it for publication was Dr. Tareq Alnaffouri. This work was supported by the National Natural Science Foundation of China under Grant 61372162. *(Corresponding author: Zhejun Lu.)*

Z. Lu is with the College of Electronic Science and Engineering, National University of Defense Technology, Changsha 410073, China, and also with the Department of Electrical and Computer Engineering, McMaster University, Hamilton, ON L8S4L8, Canada (e-mail: luzhejun@nudt.edu.cn).

W. Hu is with the College of Electronic Science and Engineering, National University of Defense Technology, Changsha 410073, China (e-mail: wdhu@nudt.edu.cn).

T. Kirubarajan is with the Department of Electrical and Computer Engineering, McMaster University, Hamilton, ON L8S4L8, Canada (e-mail: kiruba@mcmaster.ca).

Color versions of one or more of the figures in this paper are available online at http://ieeexplore.ieee.org.

Digital Object Identifier 10.1109/TSP.2017.2688960

1053-587X © 2017 IEEE. Personal use is permitted, but republication/redistribution requires IEEE permission.
See http://www.ieee.org/publications_standards/publications/rights/index.html for more information.

Authorized licensed use limited to: GUILIN UNIVERSITY OF ELECTRONIC TECHNOLOGY. Downloaded on June 22,2024 at 10:13:12 UTC from IEEE Xplore. Restrictions apply.

first order approximation, and is likely to be affected by noise and clutter [20]. Furthermore, PHD's legacy PHD cannot be correctly calculated in the presence of missed detections, leading to significant information loss. With the propagation of cardinality distribution, the CPHD filter tries to address the shortcomings of the PHD filter. Some extensions of the CPHD filter have been proposed in [21]–[24]. However, there are limitations in propagating the legacy PHD due to the "spooky action" in the PHD filter [25].

The labeled Poisson RFSs and the labeled independently and identically distributed (i.i.d.) cluster RFSs are each special cases of the generalized labeled multi-Bernoulli RFSs. Thus the labeled PHD and CPHD (LPHD and LCPHD) filters can be easily derived from the GLMB filter. However, due to moment approximation, there are difficulties in handling missed detections and extracting trajectories of targets.

In this paper, a new approach for implementing the labeled RFS with moment approximation is proposed to address these difficulties. In the LPHD and LCPHD filters, the updated PHD components are merged and the information in each component is buried in the global PHD. In order to utilize this information, the updated PHD components are separated and uniquely identified by a tag τ; accordingly, the labeled PHD and CPHD are extended to the τ-labeled PHD and τ-labeled CPHD (τ-LPHD and τ-LCPHD), respectively. Moreover, in this paper, δ-generalized labeled PHD and CPHD (δ-GLPHD and δ-GLCPHD) filtering processes are proposed for extracting states, maintaining track continuity, and modifying the legacy PHD in the τ-LPHD and τ-LCPHD, respectively. This δ-GLPHD/GLCPHD filtering formulation uses the information from the τ-LPHD/LCPHD, and, incorporated with pre-processing, reduces computational load in the association procedure. This proposed approach inherits the advantages of the δ-GLMB, with its efficient state estimation and track continuity; moreover, it saves substantial computational resources in the prediction and update procedures. Furthermore, the τ-LCPHD provides an alternative approach for missed detections that does not require enumerating an exponentially growing number of hypotheses.

The paper is organized as follows: Section II presents a review of the RFS and labeled RFS background. Section III presents the motivations and extends the labeled moment approximation RFSs. The recursion of the proposed labeled PHD and CPHD filters are given in Section IV. Simulation results are shown in Section V. Finally, conclusions are discussed in Section VI.

II. Background

This section briefly reviews the RFS and labeled RFS formulation. For more details on the descriptors, mathematical proofs, modeling, and implementations of the RFS, refer to [3], [26]; for the labeled RFS, refer to [17], [18].

A. Multitarget Bayes Filtering

In the multitarget Bayes filter, the multitarget state set and multitarget observation set are modeled as random finite sets. Suppose that at time step k, the multitarget state set and the multitarget observation set are given by $X_k \subset \mathbb{X}$ and $Z_k \subset \mathbb{Z}$, respectively. Since X_k and Z_k are random finite sets, not only do the target states evolve over time, but the number of targets varies with time as well.

The multitarget state set at time k can be modeled as

$$X_k = S_k(X_{k-1}) \cup B_k \tag{1}$$

where $S_k(X_{k-1})$ is the RFS of surviving targets with probability $p_S(\cdot)$, evolving from the previous time multitarget state set X_{k-1}, and B_k is the RFS of spontaneously newborn targets. Similarly, the multitarget observation set can be modeled as

$$Z_k = H_k(X_k) \cup \mathrm{K}_k \tag{2}$$

where $H_k(X_k)$ is the RFS of measurements generated by X_k with detection probability $p_D(\cdot)$, and K_k is the RFS of measurements from false alarms or clutter.

The multitarget Bayes predictor and corrector equations [3] are given by, respectively,

$$\pi_{k|k-1}(X_k|Z_{1:k-1}) = \int f_{k|k-1}(X_k|X)\pi_{k-1}(X|Z_{1:k-1})\delta X \tag{3}$$

$$\pi_k(X_k|Z_{1:k}) = \frac{g_k(Z_k|X_k)\pi_{k|k-1}(X_k|Z_{1:k-1})}{\int g_k(Z_k|X)\pi_{k|k-1}(X|Z_{1:k-1})\delta X} \tag{4}$$

where $\pi_{k|k-1}(\cdot|Z_{1:k-1})$, and $\pi_k(\cdot|Z_{1:k})$ are the multitarget prior and posterior density, respectively, $g_k(\cdot|\cdot)$ is the multitarget likelihood function, $f_{k|k-1}(\cdot|\cdot)$ is the multitarget Markov transition density, and $Z_{1:k} : Z_1, \ldots, Z_k$ is the measurement sets collected up to time k. The integral is a set integral of function f taking the class of finite subsets of $\mathbb{X}$, defined by

$$\int f(X)\delta X = \sum_{i=0}^{\infty} \frac{1}{i!} \int_{\mathbb{X}^i} f(\{x_1, \ldots, x_i\}) d(x_1, \ldots, x_i) \tag{5}$$

B. Multitarget Processes

Due to the computationally intractable set integral in the recursions (3)–(4), many approximations to implement the multitarget Bayes filter have been proposed. First, some fundamental descriptors of RFS are reviewed here. Let $X \subseteq \mathbb{X}$ be an RFS, and define the multi-object exponential notation h^X as

$$h^X = \begin{cases} 1 & \text{if } X = \emptyset \\ \prod_{x \in X} h(x) & \text{if } X \neq \emptyset \end{cases} \tag{6}$$

where $h(x)$ is a real-valued function with $0 \leq h(x) \leq 1$ on $x \in X$.

Let $\rho(n)$ denote the cardinality distribution, the inner product $\langle f, g \rangle \triangleq \int f(x)g(x)dx$, and let $|\cdot|$ denote the cardinality of a set. The generalized Kronecker delta function is given by

$$\delta_Y(X) \triangleq \begin{cases} 1, & \text{if } X = Y \\ 0, & \text{otherwise} \end{cases} \tag{7}$$

and the inclusion function, a generalization of the indicator function, is given by

$$1_Y(X) = \begin{cases} 1, & \text{if } X \subseteq Y \\ 0, & \text{otherwise} \end{cases} \tag{8}$$

Authorized licensed use limited to: GUILIN UNIVERSITY OF ELECTRONIC TECHNOLOGY. Downloaded on June 22,2024 at 10:13:12 UTC from IEEE Xplore. Restrictions apply.

If $X = \{x\}$, the notation $1_Y(x)$ is used in place of $1_Y(\{x\})$. Next, some multitarget processes are discussed, as follows:

1) Poisson RFSs: The PHD filter is based on the Poisson approximation. Let $v(x)$ denote the PHD (or intensity). A Poisson RFS X is one whose cardinality is Poisson distributed with mean $\langle v, 1\rangle$, i.e. $|X| \sim \text{Pois}_{\langle v,1\rangle}$, and the cardinality distribution has $\rho(n) = e^{-\langle v,1\rangle}\frac{\langle v,1\rangle^n}{n!}$. The objects in X are independent and identically distributed according to $\frac{v(\cdot)}{\langle v,1\rangle}$. The multitarget probability density is given by

$$\pi(X) = e^{-\langle v,1\rangle} v^X \tag{9}$$

2) Independent, Identically Distributed Cluster RFSs: The CPHD filter is based on the i.i.d. cluster approximation. An i.d.d. RFS X is one whose objects are independent and identically distributed according to the distribution $p(\cdot)$, and the arbitrary cardinality $\rho(\cdot)$. The multitarget probability density is given by

$$\pi(X) = |X|!\rho(|X|) \cdot p^X \tag{10}$$

3) Multi-Bernoulli RFSs: A Bernoulli RFS X has probability $1-q$ of being empty, and probability q of being a singleton that is distributed according to a spatial distribution $p(\cdot)$. The probability density is given by

$$\pi(X) = \begin{cases} 1-q & X = \emptyset \\ q \cdot p(x) & X = \{x\} \end{cases} \tag{11}$$

Thus, a multi-Bernoulli RFS is the union of a finite number N of independent Bernoulli RFSs, i.e., $X = \cup_{i=1}^{N} X^{(i)}$. The multitarget probability density of a multi-Bernoulli RFS is given by

$$\pi(X) = \prod_{i=1}^{N}(1-q^{(i)}) \sum_{1 \leqslant i_1 \neq \ldots \neq i_n \leqslant N} \prod_{j=1}^{n} \frac{q^{(i_j)} p^{(i_j)}(x_j)}{1-q^{(i_j)}} \tag{12}$$

C. Labeled RFS

The labeled RFS theory was first proposed in [17] and its implementation delineated in [18], whose unlabeled version is the same as its corresponding unlabeled RFS. Notations of the labeled RFS are briefly reviewed here.

The following convention is used with labeled RFSs. The single-object states are represented by lowercase letters, e.g., x or $\mathbf{x}$, while multi-object states are represented by uppercase letters, e.g., X or $\mathbf{X}$. Labeled states and their distributions are in bold to distinguish them from unlabeled ones, e.g., $\mathbf{x}$ or $\mathbf{X}$ or $\boldsymbol{\pi}$; spaces are represented by blackboard bold, e.g., $\mathbb{X}$, $\mathbb{Z}$, $\mathbb{L}$, $\mathbb{N}$, etc.; and the class of finite subsets of a space $\mathbb{X}$ is denoted by $\mathcal{F}(\mathbb{X})$.

The labels are drawn from a discrete label space $\mathbb{L} = \{\alpha_i : i \in \mathbb{N}\}$, where $\mathbb{N}$ is the set of positive integers and α_i are distinct. A labeled RFS with state space $\mathbb{X}$ and label space $\mathbb{L}$ is an RFS on $\mathbb{X} \times \mathbb{L}$. The label set of $\mathbf{X}$ is given by $\mathcal{L}(\mathbf{X}) = \{\mathcal{L}(\mathbf{x}), \mathbf{x} \in \mathbf{X}\}$, where the projection $\mathcal{L} : \mathbb{X} \times \mathbb{L} \to \mathbb{L}$ is defined as $\mathcal{L}((x,\ell)) = \ell$. Each labeled RFS realization $\mathbf{X}$ must have distinct label $|\mathcal{L}(\mathbf{X})| = |\mathbf{X}|$. The distinct label indicator, which is used to ensure distinct labels, is given by

$$\Delta(\mathbf{X}) \triangleq \delta_{|\mathbf{X}|}(|\mathcal{L}(\mathbf{X})|) \tag{13}$$

The unlabeled version of a labeled RFS can be obtained by the projection from $\mathbb{X} \times \mathbb{L}$ into $\mathbb{X}$. Furthermore, the unlabeled version and the labeled version of an RFS have the same cardinality distribution. The unlabeled version of a labeled RFS is distributed according to

$$\pi(\{x_1, \ldots, x_n\}) = \sum_{(\ell_1,\ldots,\ell_n)\in\mathbb{L}^n} \pi(\{(x_1,\ell_1),\ldots,(x_n,\ell_n)\}) \tag{14}$$

Some labeled RFSs are given as follows:

1) Labeled Poisson RFSs: The density of a labeled Poisson RFS, based on the Poisson distribution $\text{Pois}_\lambda(n) = e^{-\lambda}\lambda^n/n!$, is given by

$$\pi(\{(x_1,\ell_1),\ldots,(x_n,\ell_n)\}) = \delta_{\mathbb{L}(n)}(\{\ell_1,\ldots,\ell_n\})\text{Pois}_{\langle v,1\rangle}(n)\prod_{i=1}^{n}\frac{v(x_i)}{\langle v,1\rangle} \tag{15}$$

2) Labeled i.d.d. Cluster RFSs: A labeled i.i.d. cluster RFS generalizes the Poisson distribution to cardinality distribution $\rho(n)$, whose density is given by

$$\pi(\{(x_1,\ell_1),\ldots,(x_n,\ell_n)\}) = \delta_{\mathbb{L}(n)}(\{\ell_1,\ldots,\ell_n\})\rho(n)\prod_{i=1}^{n}\frac{v(x_i)}{\langle v,1\rangle} \tag{16}$$

3) Labeled Multi-Bernoulli RFSs: In a labeled multi-Bernoulli RFS, the parameter set $\{(q^{(\zeta)}, p^{(\zeta)}) : \zeta \in \Psi\}$ has the same meaning in a multi-Bernoulli RFS. The density of the labeled multi-Bernoulli RFS is given by

$$\pi(\{(x_1,\ell_1),\ldots,(x_n,\ell_n)\}) = \delta_n(|\{\ell_1,\ldots,\ell_n\}|)\times \prod_{\zeta\in\Psi}(1-q^{(\zeta)}) \times \prod_{j=1}^{n}\frac{1_{\alpha(\Psi)}(\ell_j)q^{(\alpha^{-1}(\ell_j))}p^{(\alpha^{-1}(\ell_j))}(x_j)}{1-q^{(\alpha^{-1}(\ell_j))}} \tag{17}$$

where $\alpha : \Psi \to \mathbb{L}$ is a one-to-one mapping.

D. Generalized Labeled Multi-Bernoulli RFSs

The generalized labeled multi-Bernoulli RFS is closed under the Chapman-Kolmogorov equation [17]. That is to say, if the prior distribution is a generalized labeled multi-Bernoulli, then, under the standard multi-object likelihood function, the posterior distribution is also a generalized labeled multi-Bernoulli.

A generalized labeled multi-Bernoulli RFS is a labeled RFS on $\mathbb{X} \times \mathbb{L}$ distributed according to

$$\pi(\mathbf{X}) = \Delta(\mathbf{X})\sum_{c\in\mathbb{C}} w^{(c)}(\mathcal{L}(\mathbf{X}))\left[p^{(c)}\right]^{\mathbf{X}} \tag{18}$$

where $\mathbb{C}$ is a discrete index set, and the weights $w^{(c)}(L)$ and the spatial distributions $p^{(c)}$ satisfy

$$\sum_{L\subseteq\mathbb{L}}\sum_{c\in\mathbb{C}} w^{(c)}(L) = 1 \tag{19}$$

$$\int p^{(c)}(x,\ell)dx = 1 \tag{20}$$

Authorized licensed use limited to: GUILIN UNIVERSITY OF ELECTRONIC TECHNOLOGY. Downloaded on June 22,2024 at 10:13:12 UTC from IEEE Xplore. Restrictions apply.

The GLMB density can be interpreted as a mixture of multi-object exponentials. In each term of (18), $w^{(c)}(\mathcal{L}(\mathbf{X}))$ is the weight that depends on the labels of the multi-object state, and $\left[p^{(c)}\right]^{\mathbf{X}}$ is the multi-object exponential that depends on the entire multi-object state.

The sum over $c \in \mathbb{C}$ in the definition of the GLMB can be interpreted as all possible data association hypotheses. Since the number of hypotheses grows exponentially with time, it is necessary to reduce the number of components by discarding insignificant hypotheses.

E. δ-Generalized Labeled Multi-Bernoulli

A computationally efficient version of the GLMB called δ-generalized labeled multi-Bernoulli (δ-GLMB) is proposed in [17], [18]. The δ-GLMB is a special case of a generalized labeled multi-Bernoulli RFS on $\mathbb{X} \times \mathbb{L}$ with

$$\mathbb{C} = \mathcal{F}(\mathbb{L}) \times \Xi$$
$$w^{(c)}(L) = w^{(I,\xi)}(L) = w^{(I,\xi)}\delta_I(L)$$
$$p^{(c)} = p^{(I,\xi)} = p^{(\xi)}$$

where Ξ is a discrete space, each $\xi \in \Xi$ represents a history of association maps, and $I \in \mathcal{F}(\mathbb{L})$ represents a set of tracks labels. The density of a δ-GLMB RFS is given by

$$\pi(\mathbf{X}) = \Delta(\mathbf{X}) \sum_{(I,\xi)\in\mathcal{F}(\mathbb{L})\times\Xi} w^{(I,\xi)}\delta_I(\mathcal{L}(\mathbf{X}))\left[p^{(\xi)}\right]^{\mathbf{X}} \quad (21)$$

The cardinality distribution and PHD of a GLMB are given by, respectively,

$$\rho(n) = \sum_{(I,\xi)\in\mathcal{F}_n(\mathbb{L})\times\Xi} w^{(I,\xi)} \quad (22)$$

$$v(x) = \sum_{\ell\in\mathbb{L}} \sum_{(I,\xi)\in\mathcal{F}(\mathbb{L})\times\Xi} w^{(I,\xi)} 1_I(\ell) p^{(\xi)}(x,\ell) \quad (23)$$

The δ-GLMB can be implemented by truncating the weighted sums of multitarget exponentials in prediction and update operations, without computing all components. The multitarget posterior and prediction densities are truncated using the ranked assignment and K-shortest paths algorithms, respectively [18]. A recent implementation of the GLMB filter combines the prediction and update into a single step with a new truncation technique based on Gibbs sampling that reduces the complexity [27].

III. Extensions for Labeled Moment Approximation RFSs

A. Labeled Moment Approximation RFSs

The labeled Poisson and i.d.d. cluster RFSs are special cases of the GLMB RFS, with only one element in the index space $\mathbb{C}$. Thus, the superscript (c) in (18) is unnecessary, and the following form of the density of the labeled Poisson or i.d.d. cluster RFS can be obtained:

$$\pi(X) = \Delta(X) w(\mathcal{L}(X)) p^X \quad (24)$$

The weights $w(L)$ and spatial distributions $p(x,\ell)$ are written as, respectively,

$$w(L) = \delta_{\mathbb{L}(|L|)}(L)\mathrm{Pois}_{\langle v,1\rangle}(|L|) \quad (25)$$

$$p(x,\ell) = v(x)/\langle v,1\rangle \quad (26)$$

The labeled Poisson RFS can be generalized to the labeled i.i.d. cluster RFS by removing the Poisson assumption on the cardinality and specifying an arbitrary cardinality distribution $\rho(n)$. The weights $w(L)$ and spatial distributions $p(x,\ell)$ are given by, respectively,

$$w(L) = \delta_{\mathbb{L}(|L|)}(L)\rho(|L|) \quad (27)$$

$$p(x,\ell) = v(x)/\langle v,1\rangle \quad (28)$$

B. Issues in Moment Approximation

Even though the formulation of the labeled PHD/CPHD (LPHD/LCPHD) is elegant and computational tractable, it still has issues that need to be addressed. The principle issues are discussed below.

- Approximation of spatial distribution — In the LPHD/LCPHD filtering process, the multitarget posterior is approximated to be Poisson and i.d.d. cluster distributions, respectively. This approximation confuses the posterior density of each track. If tracks are well separated, this approximation can be valid. But, when objects are closely-spaced, the state and cardinality estimates become unstable, since the minor modes derived from the associations between unrelated measurements and tracks will affect the PHD distribution.
- Difficulties with extracting states and maintaining track continuity — Since all tracks are assumed to be independent and identically distributed, the objects are not distinguished by the filter. The states of objects are buried in the global spatial distribution, and thus it is difficult to extract their state. Furthermore, track continuity cannot be maintained by extracting trajectories of the objects.
- Weakness in dealing with missed detections — The LPHD propagates the legacy PHD $v_L(x) = (1 - p_D(x))v(x)$ to the next time step, resulting in information loss similar to the standard PHD filter [28]. In the LCPHD, the legacy PHD cannot be distributed to corresponding tracks, suffering from the "spooky effect" [25]. This is an inevitable result of the i.d.d. approximation.
- Response to newborn targets — Because of the resilience of the LCPHD with respect to target appearances and disappearances, the LCPHD has a smaller transient response to newborn targets, similar to the standard CPHD filter [3]. Furthermore, the more targets there are in the scenario, the slower the response of the LCPHD to target appearances and disappearances. In some cases this does not constitute a weakness, especially for the missed targets. But, due to the moment approximation, if there are simultaneous newborn targets and missed detections, the filter may not yield the correct legacy cardinality.

Authorized licensed use limited to: GUILIN UNIVERSITY OF ELECTRONIC TECHNOLOGY. Downloaded on June 22,2024 at 10:13:12 UTC from IEEE Xplore. Restrictions apply.

C. τ-Labeled Moment Approximation RFS

To address the issues in moment approximation, an extra tag τ is introduced into the LPHD/LCPHD to mark PHD components that belong to different tracks, and the LPHD/LCPHD are extended to the τ-LPHD/LCPHD.

In the PHD/CPHD update, since all tracks buried in global PHD are jointly updated by each measurement [3], the PHD components are aggregated by measurements. In the extended formulation, each PHD component is maintained separately and marked by an integer triplet $\tau = (k, m, n)$, where k is the appearance time step of measurement, m is the index of measurement z_m, and n is an index to distinguish different τ with the same m. The space of τ is represented by $\mathbb{T}$. The updated PHD components marked by the new τ should be unique, to distinguish them from legacy PHD components. The newborn PHD components are marked by the new $\tau_B = (k, m, n)$ with $m = \alpha_{B,i}, i \in \mathbb{N}$; all $\alpha_{B,i}$ are new distinct positive integers. The parameter, e.g. m, in $\tau = (k, m, n)$, is represented as $m(\tau)$ by convention. It is still called "*track*," since it contains the posterior of the association between tracks and measurements.

D. δ-Generalized Extension

Moreover, in order to address the issues of maintaining track continuity and handling the missed detections, a generalization of the LPHD/LCPHD is needed. The computational cost of the δ-GLMB filter is the main obstacle in its implementation. Based on the information from the τ-LPHD/LCPHD, a computationally efficient δ-generalized extension is proposed.

This extension is similar to the δ-GLMB recursion, but the PHD components from τ-LPHD/LCPHD are used instead of prior and posterior distributions. The prior and posterior distributions do not need to be calculated in every hypothesis, based on the following property:

Reusable components: The weights and spatial distributions calculated in the δ-GLMB prediction and updated components can be used repeatedly in different hypotheses.

These components can be calculated from the PHD components of τ-LPHD/LCPHD and reused in different hypotheses to save computation time. The approach to distinguish different PHD components in different hypotheses is based on the following property:

Exclusive components: The updated components of a measurement from different tracks are mutually exclusive, since only one track is correctly associated with this measurement, and the other components from incorrect association are interferences and buried in the global PHD.

Thus, in each association hypothesis, the PHD components with different $m(\tau)$ can coexist, while those with the same $m(\tau)$ are mutually exclusive. Thus, the label ℓ in each hypothesis has its relevant and distinct τ according to $\tau = \sigma(\ell)$, where $\sigma : I \to T$ is a one-to-one mapping, where I and T are the set of ℓ and set of τ of the hypothesis, respectively. Since it inherits the advantages of δ-GLMB, and in order to distinguish it from PHD and CPHD, this approach is called δ-generalized labeled PHD/CPHD.

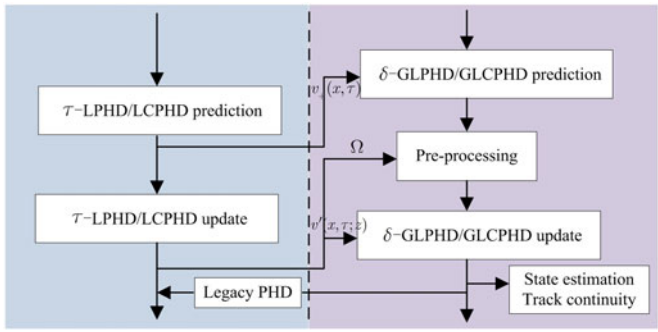

Fig. 1. The proposed labeled PHD and CPHD recursion.

Based on the information from the τ-LPHD/LCPHD, the δ-GLPHD/GLCPHD is operated in parallel to extract states, maintain track continuity, and modify the legacy PHD.

IV. The Labeled PHD and CPHD Recursion

The detailed description of the proposed LPHD/LCPHD recursion are given in this section. The illustration of the recursion is summarized in Figure 1, and the corresponding pseudo-code is given in Appendix VI.

A. τ-LPHD/LCPHD Prediction

The density of the τ-LPHD/LCPHD has the same form as LPHD/LCPHD, which is given by

$$\boldsymbol{\pi}(\mathbf{X}) = \Delta(\mathbf{X}) w(\mathcal{L}(\mathbf{X})) p^{\mathbf{X}} \tag{29}$$

Suppose that the multi-object posterior density is an LPHD/LCPHD with state space $\mathbb{X}$, label space $\mathbb{L}$, and PHD $v(x)$, and that the multi-object birth model is an LPHD/LCPHD with state space $\mathbb{X}$, label space $\mathbb{B}$ and PHD $v_B(x)$, then the predicted multi-object density is an LPHD/LCPHD with state space $\mathbb{X}$, label space $\mathbb{L}_+ = \mathbb{L} \cup \mathbb{B}$, and PHD $v_+(x)$, given by

$$\boldsymbol{\pi}_+(\mathbf{X}_+) = \Delta(\mathbf{X}_+) w(\mathcal{L}(\mathbf{X}_+)) p_+^{\mathbf{X}} \tag{30}$$

In the LPHD, one has

$$w(L) = \delta_{\mathbb{L}_+(|L|)}(L) \mathrm{Pois}_{\langle v_+, 1\rangle}(|L|) \tag{31}$$

$$p_+(x, \ell) = v_+(x) / \langle v_+, 1\rangle \tag{32}$$

$$v_+(x) = v_{+,S}(x) + v_B(x) \tag{33}$$

$$v_{+,S}(x) = \langle p_S(\cdot, \ell) f(x|\cdot), v(\cdot)\rangle \tag{34}$$

This prediction process is similar to the prediction process in the standard PHD filter [8]. While in the LCPHD, the $p_+(x, \ell)$ and $v_+(x)$ have the same form, and the weights have

$$w(L) = \delta_{\mathbb{L}_+(|L|)}(L) \rho_+(|L|) \tag{35}$$

where the predicted cardinality distribution $\rho_+(n)$ is given by [9],

$$\rho_+(n) = \sum_{j=0}^{n} \rho_B(n-j) \sum_{l=j}^{\infty} C_j^l \frac{\langle p_{S,k}, v\rangle^j \langle 1 - p_{S,k}, v\rangle^{l-j}}{\langle 1, v\rangle^l} \rho(l) \tag{36}$$

where C_j^n is the combinatorial coefficient $C_j^n = \frac{n!}{j!(n-j)!}$.

Authorized licensed use limited to: GUILIN UNIVERSITY OF ELECTRONIC TECHNOLOGY. Downloaded on June 22,2024 at 10:13:12 UTC from IEEE Xplore. Restrictions apply.

The difference between the τ-LCPHD/LPHD and the LCPHD/LPHD is that the PHD components in $v_+(x)$ are separated by distinct marks τ. The PHD of the predicted τ-LPHD/LCPHD is a labeled moment approximation on the space of $\mathbb{X}\times\mathbb{T}_+$, where $\mathbb{T}_+=\mathbb{T}\cup\mathbb{T}_B$. The surviving PHD has $v_{+,S}(x)=\sum_{\tau\in\mathbb{T}}v_{+,S}(x,\tau)$ and newborn PHD has $v_B(x)=\sum_{\tau_B\in\mathbb{T}_B}v_B(x,\tau_B)$, thus,

$$v_+(x)=\sum_{\tau\in\mathbb{T}}v_{+,S}(x,\tau)+\sum_{\tau_B\in\mathbb{T}_B}v_B(x,\tau_B) \tag{37}$$

B. τ-LPHD/LCPHD Update

If the multi-object prior has the form of (30), and clutter is modeled by a Poisson RFS with intensity function $\kappa(\cdot)$, then the multi-object posterior is an LPHD/LCPHD, given by

$$\boldsymbol{\pi}(\mathbf{X}|Z)=\Delta(\mathbf{X})w(\mathcal{L}(\mathbf{X}))[p(\cdot|Z)]^{\mathbf{X}} \tag{38}$$

In the LPHD, one has

$$w(L)=\delta_{\mathbb{L}_+(|L|)}(L)\mathrm{Pois}_{\langle v(\cdot|Z),1\rangle}(|L|) \tag{39}$$

$$p(x,\ell)=v(x|Z)/\langle v(\cdot|Z),1\rangle \tag{40}$$

$$v'(x;z)=p_D(x)g(z|x)v_+(x) \tag{41}$$

$$v(x|Z)=\sum_{z\in Z}\frac{v'(x;z)}{\kappa(z)+\langle p_D(x)g(z|x),v_+(x)\rangle} \tag{42}$$

In the LCPHD, let P_j^n denote the permutation coefficient $P_j^n=\frac{n!}{(n-j)!}$, and $e_j(Z)$ the jth degree elementary symmetric function defined as

$$e_j(Z)=\sum_{Y\subseteq Z,|Y|=j}\left(\prod_{y\in Y}y\right)$$

and by convention $e_0(Z)=1$.

Thus, the update equations of LCPHD are given by

$$w(L)=\delta_{\mathbb{L}_+(|L|)}(L)\rho_Z(|L|) \tag{43}$$

$$p(x,\ell)=v(x|Z)/\langle v(\cdot|Z),1\rangle \tag{44}$$

$$v(x|Z)=\sum_{z\in Z}\frac{\left\langle\Upsilon_k^1[v_+,Z\backslash\{z\}],\rho_+\right\rangle}{\langle\Upsilon_k^1[v_+,Z],\rho_+\rangle}\phi_z(x) \tag{45}$$

$$\rho_Z(n)=\frac{\Upsilon_k^1[v_+,Z](n)\rho_+(n)}{\langle\Upsilon_k^1[v_+,Z],\rho_+\rangle} \tag{46}$$

where

$$\Upsilon_k^u[v,Z](n)=\sum_{j=0}^{\min(|Z|,n)}(|Z|-j)!\rho_{\mathrm{K},k}(|Z|-j)P_{j+u}^n\times \frac{\langle 1-p_D,v\rangle^{n-(j+u)}}{\langle 1,v\rangle^n}e_j(\Xi_k(\phi,Z)) \tag{47}$$

$$\Xi_k(\phi,Z)=\{\langle\phi_z(\cdot),1\rangle:z\in Z\} \tag{48}$$

$$\phi_z(x)=\frac{\langle 1,\kappa\rangle}{\kappa(z)}v'(x;z) \tag{49}$$

$$v'(x;z)=p_D(x)g(z|x)v_+(x) \tag{50}$$

The PHD of the updated τ-LPHD/LCPHD is a labeled moment approximation on the space of $\mathbb{X}\times\mathbb{T}$, given by

$$v(x|Z)=\sum_{\tau\in\mathbb{T}_+}v(x,\tau|Z)=\sum_{\tau\in\mathbb{T}_+}\sum_{z\in Z}v(x,\tau;z) \tag{51}$$

and

$$v'(x;z)=\sum_{\tau\in\mathbb{T}_+}v(x,\tau;z) \tag{52}$$

where $v'(x;z)$ is used in the δ-GLPHD/GLCPHD.

The "*weight*" is used to represent the integral of the corresponding PHD as $r(\tau)=\langle v(\cdot,\tau),1\rangle$, and $r(\tau;z)=\langle v(\cdot,\tau;z),1\rangle$. The integral of PHD over a region is the expected number of targets in that region, and the weight is the integral of intensity density. Thus, the sum of the weights of certain tracks can be considered proportional to the intensity of existing targets.

Remark 1: The greater the sum of the weights of certain tracks, the higher the probability that targets exist.

Last, the $\tau\in\mathbb{T}_+$ in measurement-updated $v(x,\tau;z)$ is rewritten as new $\tau\in\mathbb{T}_Z$ in $v(x,\tau)$, where $\mathbb{T}_Z$ is a new space in which τ is generated from measurement $z\in Z$ at this time. Thus, space $\mathbb{T}$ consists of both legacy space $\mathbb{T}_+$ and new space $\mathbb{T}_Z$, becoming $\mathbb{T}=\mathbb{T}_+\cup\mathbb{T}_Z$. The legacy PHD is considered in subsection IV-F.

C. Computation Load Reduction Pre-processing

A number of partitioning methods have been proposed to make the filtering process more efficient [11], [19], [29]. A simple and effective partitioning procedure is used here to considerably reduce the computational load.

The notation Γ is used to represent the set of τ with same $m(\tau)$ (from the same measurement). For simplicity, the sum of the PHD components of τ in Γ is written as $v(x,\Gamma)=\sum_{\tau\in\Gamma}v(x,\tau)$, and the measurement-updated PHD from τ in Γ is written as $v(x,\Gamma;z)=\sum_{\tau\in\Gamma}v(x,\tau;z)$.

Let $W_{i,j}$ denote the weight contribution from track $\tau_i\in\mathbb{T}_+$ to measurement $z_j\in Z$, which can be calculated by

$$W_{i,j}\triangleq r(\Gamma_i;z_j)=\sum_{\tau\in\Gamma_i}\langle v(\cdot,\tau;z_j),1\rangle \tag{53}$$

The measurement-updated weight can be written as

$$r(z_j)=\sum_{\tau\in\mathbb{T}_+}r(\tau;z_j)=\sum_{\Gamma\subseteq\mathbb{T}_+}r(\Gamma;z_j)=\sum_i W_{i,j} \tag{54}$$

The updated weight generated from tracks $\tau\in\Gamma$ can be written as

$$r_U(\Gamma)=\sum_{z\in Z}\sum_{\tau\in\Gamma}r(\tau;z)=\sum_{\Gamma\subseteq\mathbb{T}_+}r(\Gamma;z)=\sum_j W_{i,j} \tag{55}$$

Suppose that, at this time, there are M sets of Γ. The weight contribution matrix is given in Table I. This matrix can be decomposed into a number of smaller ones. Pre-processing proceeds based on the following property:

"Self-gating" property: If a measurement is consistent with prior information, this measurement contributes one target to

Authorized licensed use limited to: GUILIN UNIVERSITY OF ELECTRONIC TECHNOLOGY. Downloaded on June 22,2024 at 10:13:12 UTC from IEEE Xplore. Restrictions apply.

TABLE I
WEIGHT CONTRIBUTION MATRIX

Ω	z_1	z_2	$\cdots$	$z_{\lvert Z\rvert}$
Γ_1	$W_{1,1}$	$W_{1,2}$	$\cdots$	$W_{1,\lvert Z\rvert}$
Γ_2	$W_{2,1}$	$W_{2,2}$	$\cdots$	$W_{2,\lvert Z\rvert}$
$\vdots$	$\vdots$	$\vdots$	$\ddots$	$\vdots$
Γ_M	$W_{M,1}$	$W_{M,2}$	$\cdots$	$W_{M,\lvert Z\rvert}$

the cardinality estimate, while for clutter, it contributes almost nothing to the cardinality estimate. This fact is also interpreted as the "self-gating" property of the PHD and CPHD filters in [3].

Thus, this property can be used to distinguish between targets and clutter. Moreover, if a measurement is generated from a target, the larger the weight contribution from the track to this measurement, the higher the probability that this measurement is generated from the track. The pre-processing is summarized as follows:

1) For clutter, one has $r(z) \approx 0$, hence measurement z with $r(z) < \vartheta_c$ is considered to be clutter and its corresponding PHD is discarded.
2) If $W_{i,j} < \vartheta_d$, measurement z_j is considered to be not from track $\tau \in \Gamma_i$. The corresponding PHD components $v(x,\tau;z_j), \tau \in \Gamma_i$ are discarded; set $W_{i,j} = 0$.
3) If $W_{i,j} > \vartheta_r$ and $\sum_l W_{i,l} - W_{i,j} > \vartheta_c$, measurement z_j is considered to be derived from track $\tau \in \Gamma_i$, and PHD components $v(x,\tau;z_j), \tau \in \Gamma_i$ are considered to be the updated PHD and normalized to $v(x;z_j) = \sum_{\tau\in\mathbb{T}_+} v(x,\tau;z)$. The other PHD components $v(x,\tau;z_j), \tau \notin \Gamma_i$ are discarded.

The ϑ_c, ϑ_d, and ϑ_r mentioned above are preset thresholds. The partitioning procedure is to group the closely-spaced tracks with their possible associated measurements, and process each group separately. The following function is used for the partitioning process:

Define a function β, and $\beta(\Gamma_i)$ indicates

$$\beta(\Gamma_i) = \{z_{m_1}, z_{m_2}, \ldots, z_{m_P}\} \tag{56}$$

where $W_{i,m_1} \neq 0, W_{i,m_2} \neq 0, \ldots, W_{i,m_P} \neq 0$, and P denotes the number of non-zero W terms in Γ_i.

If $\beta(\Gamma_i) \cap \beta(\Gamma_l) \neq \emptyset$, the sets Γ_i and Γ_l belong to same group. Otherwise, sets Γ_i and Γ_l belong to different groups. The measurement set associated to these two sets is given by $Z^{(\Gamma_i,\Gamma_l)} = \beta(\Gamma_i) \cup \beta(\Gamma_l)$.

First, function β is used for all Γ. Next, those Γ that have $\beta(\Gamma_i) \cap \ldots \cap \beta(\Gamma_l) \neq \emptyset$ are grouped together, and the corresponding measurement set for this group is formed by $\beta(\Gamma_i) \cup \ldots \cup \beta(\Gamma_l)$. Finally, the tracks τ in different Γ and measurements z are divided into different groups $\{\Omega_n\}_{n=1}^N$, and only the associations between the measurements and tracks in the same matrix need to be considered. The apparent unrelated tracks and measurements will not be in the same matrix. Figure 2 illustrates an example of the partitioning process.

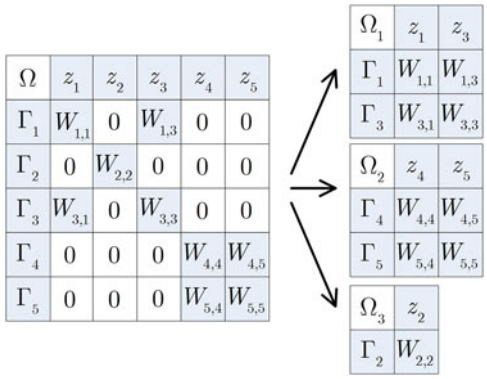

Fig. 2. An example of the partitioning process.

D. δ-Generalized Labeled PHD/CPHD Prediction

Input:

$$\{(I^{(h)}, \sigma^{(h)}, \xi^{(h)}, w^{(h)}, v^{(h)}, K^{(h)}\}_{h=1}^{H}$$

Output:

$$\{(I_+^{(h,j,b)}, \sigma_+^{(h,j,b)}, w_+^{(h,j,b)}, v_+^{(h,j,b)}\}_{(h,j,b)=(1,1)}^{(H,K^{(h)},K_B)}$$

Given the input enumerated parameter set, the prediction density is given by

$$\boldsymbol{\pi}_+(\mathbf{X}_+) = \sum_{h=1}^{H} \hat{\pi}_+^{(h)}(\mathbf{X}_+) \tag{57}$$

where $\hat{\boldsymbol{\pi}}_+^{(h)}(\mathbf{X}_+)$ is the truncated version of $\boldsymbol{\pi}_+^{(h)}(\mathbf{X}_+)$ with the following form

$$\boldsymbol{\pi}_+^{(h)}(\mathbf{X}_+) = \Delta(\mathbf{X}_+) \sum_{j=1}^{K^{(h)}} \sum_{b=1}^{K_B} w_+^{(h,j,b)} \delta_{J^{(h,j)}\cup L^{(b)}}(\mathcal{L}(\mathbf{X}_+)) \left[p_+^{(h)}\right]^{\mathbf{X}_+} \tag{58}$$

For newborn targets, a labeled multi-Bernoulli birth model is used with track weight $r_B^{(\ell)}$. The components of the $\hat{\boldsymbol{\pi}}_+^{(h)}(\mathbf{X}_+)$ are calculated based on the information from the τ-LPHD/LCPHD, given by

$$I_+^{(h,j,b)} = J^{(h,j)} \cup L^{(b)} \tag{59}$$

$$w_B^{(b)} = \prod_{\ell\in L^{(b)}} r_B^{(\ell)} \prod_{\ell\in\mathbb{B}-L^{(b)}} [1 - r_B^{(\ell)}] \tag{60}$$

$$w_+^{(h,j,b)} = w^{(h)} \left[\eta_S^{(h)}\right]^{J^{(h,j)}} \left[1 - \eta_S^{(h)}\right]^{I^{(h)}-J^{(h,j)}} w_B^{(b)} \tag{61}$$

$$p_+^{(h)}(x,\ell) = 1_{\mathbb{L}}(\ell) \frac{v_{+,S}^{(h)}(x,\ell)}{\left\langle v_{+,S}^{(h)}(\cdot,\ell), 1\right\rangle} + 1_{\mathbb{B}}(\ell) \frac{v_B^{(h)}(x,\ell)}{\left\langle v_B^{(h)}(\cdot,\ell), 1\right\rangle} \tag{62}$$

$$\eta_S^{(h)}(\ell) = \frac{\left\langle v_{+,S}^{(h)}(\cdot,\ell), 1\right\rangle}{\left\langle v^{(h)}(\cdot,\ell), 1\right\rangle} \tag{63}$$

Authorized licensed use limited to: GUILIN UNIVERSITY OF ELECTRONIC TECHNOLOGY. Downloaded on June 22,2024 at 10:13:12 UTC from IEEE Xplore. Restrictions apply.

The subsets generated from $I^{(h)}$ with association map history $\xi^{(h)}$ are surviving label sets $\{J^{(h,j)}\}_{j=1}^{K^{(h)}}$, and the subsets generated from $\mathbb{B}$ are birth label sets $\{L^{(b)}\}_{b=1}^{K_B}$. The number of subsets $K^{(h)}$ and K_B are determined based on the analysis of the updated PHD generated from track τ. The mapping $\sigma^{(h,j,b)} = \sigma^{(h,j)} \cup \sigma^{(b)}$, where $\sigma^{(h,j)} = J^{(h,j)} \to T^{(h,j)}$ and $\sigma^{(b)} = L^{(b)} \to T^{(b)}$. Based on mapping $\sigma^{(h,j)}$, the PHD component $v_+^{(h)}(x,\ell)$ is $v_+(x,\tau)$, where $\tau = (\sigma^{(h,j)})^{-1}(\ell)$, given by the τ-LPHD/LCPHD prediction. Based on Remark 1, the updated weight of a track can be considered proportional to its existing probability.

Remark 2: The larger the updated weight $r_U(\Gamma)$ from track $\tau \in \Gamma$, the higher the probability that this track exists in this time.

Thus, if $r_U(\Gamma) > \vartheta_s, \tau \in \Gamma$, where ϑ_s is a preset threshold, the track $\ell = \sigma^{-1}(\tau)$ is considered existing, and its predicted weight is $\eta_S(\ell)$; otherwise, its predicted weights have two alternatives: $\eta_S(\ell)$ and $1 - \eta_S(\ell)$.

Consequently, the number of requested subsets are $K^{(h)} = 1^{n_1} 2^{n_2}$ and $K^{(b)} = 2^{n_B}$, where n_1 is the number of existing tracks under consideration, n_2 is the number of tracks whose state is uncertain ("state uncertain tracks"), and n_B is the number of newborn tracks. Since the prediction components that generate significant update components can be known in advance, the prediction process based on these prediction components saves substantial computations. Furthermore, if the number of requested components is still large, the K-shortest paths algorithm can be used to select the K most significant hypotheses [30], instead of enumerating all [18].

E. δ-Generalized Labeled PHD/CPHD Update

Input:

$$\{(I^{(h)}, \sigma^{(h)}, \xi^{(h)}, w^{(h)}, v^{(h)}, M^{(h)}\}_{h=1}^{H}$$

Output:

$$\{(I^{(h,j)}, \sigma^{(h,j)}, \xi^{(h,j)}, w^{(h,j)}, v^{(h,j)}\}_{(h,j)=(1,1)}^{(H,G^{(h)})}$$

Given the prediction enumerated parameter set, the posterior density is given by

$$\pi(\mathbf{X}|Z) = \sum_{h=1}^{H} \hat{\pi}^{(h)}(\mathbf{X}|Z) \tag{64}$$

where $\hat{\pi}^{(h)}(\mathbf{X}|Z)$ is the truncated version of $\pi^{(h)}(\mathbf{X}|Z)$ with the following form

$$\hat{\pi}^{(h)}(\mathbf{X}|Z) = \Delta(\mathbf{X}) \sum_{j=1}^{G^{(h)}} w^{(h,j)} \delta_{I^{(h)}}(\mathcal{L}(\mathbf{X})) \left[p^{(h,j)}\right]^{\mathbf{X}} \tag{65}$$

and

$$w^{(h,j)} = w^{(h)} [\eta_Z^{(h,j)}]^{I^{(h)}} \tag{66}$$

$$p^{(h,j)}(x,\ell|Z) = \frac{\psi_Z(x,\ell;\theta^{(h,j)})}{\eta_Z^{(h,j)}(\ell)} \tag{67}$$

$$\eta_Z^{(h,j)}(\ell) = \left\langle \psi_Z(\cdot,\ell;\theta^{(h,j)}), 1 \right\rangle \tag{68}$$

$$r^{(h,j)}(\ell; z_{\theta^{(h,j)}}) = \left\langle v^{(h,j)}(\cdot,\ell; z_{\theta^{(h,j)}}), 1 \right\rangle \tag{69}$$

$$\psi_Z(x,\ell;\theta^{(h,j)}) = \begin{cases} \dfrac{v^{(h,j)}(x,\ell; z_{\theta^{(h,j)}})}{\kappa(z_{\theta^{(h,j)}}) r^{(h,j)}(\ell; z_{\theta^{(h,j)}})} & \theta^{(h,j)}(\ell) > 0 \\ \dfrac{v_+^{(h)}(\cdot,\ell)(1 - p_D(x,\ell))}{\left\langle v_+^{(h)}(\cdot,\ell), 1 \right\rangle} & \theta^{(h,j)}(\ell) = 0 \end{cases} \tag{70}$$

The components of the $\hat{\pi}^{(h)}(\mathbf{X}|Z)$ are calculated based on the information from the τ-LPHD/LCPHD. The mapping $\sigma^{(h,j)} = I^{(h,j)} \to T^{(h,j)}$, where $I^{(h,j)} = I^{(h)}$, $T^{(h,j)} = T^{(h)} \cup T_Z^{(j)}$, and $T_Z^{(j)}$ is the set of new distinct τ with respect to current measurements. Based on the mapping $\sigma^{(h,j)}$, the PHD $v^{(h,j)}(x,\ell; z_{\theta^{(h,j)}})$ is $v'(x,\tau; z_{\theta^{(h,j)}})$, where $\tau = (\sigma^{(h,j)})^{-1}(\ell)$, given by the τ-LPHD/LCPHD update.

The updated history of association maps $\xi^{(h,j)}$ consists of the prior $\xi^{(h)}$ and new association map $\theta^{(h,j)}$. Each association map $\theta \in \Theta$, where Θ is the association map space, can be represented by an association matrix S with size $|I| \times |Z|$ that consists of 0 or 1 entries. For $i \in \{1,\ldots,|I|\}$, $j \in \{1,\ldots,|Z|\}$, $S_{i,j} = 1$ if and only if the jth measurement is assigned to track ℓ_i, i.e., $\theta(\ell_i) = j$. The sum of every row and column has $\sum_j S_{i,j} \le 1$ and $\sum_i S_{i,j} \le 1$, respectively. A row with $\sum_j S_{i,j} = 0$ means that track ℓ_i is misdetected, and a column with $\sum_i S_{i,j} = 0$ means that measurement z_j is clutter.

The cost matrix $C_Z^{(h)}$ in h is an $|I^{(h)}| \times |Z|$ matrix with entries $C_{i,j}$ given by

$$C_{i,j} = -\ln\left(\frac{\left\langle v^{(h,\cdot)}(\cdot,\ell_i; z_j), 1 \right\rangle}{\left\langle v_+^{(h)}(\cdot,\ell_i), 1 - p_D(\cdot,\ell_i) \right\rangle \kappa(z_j)}\right) \tag{71}$$

The cost of an assignment matrix is given by

$$\Im^{(h,j)} = \sum_{i=1}^{|I^{(h)}|} \sum_{j=1}^{|Z|} C_{i,j} S_{i,j} \tag{72}$$

Thus, the $[\eta_Z^{(h,j)}]^{I^{(h)}}$ in hypothesis weight $w^{(h,j)}$ can be calculated by

$$\left[\eta_Z^{(h,j)}\right]^{I^{(h,j)}} = \exp(-\Im^{(h,j)}) \prod_{\ell \in I^{(h)}} \frac{\left\langle v^{(h)}(\cdot,\ell), 1 - p_D(\cdot,\ell) \right\rangle}{\left\langle v^{(h)}(\cdot,\ell), 1 \right\rangle} \tag{73}$$

With cost matrix $C_Z^{(h)}$, the subsets generated in h are $\{\theta^{(h,j)}\}_{j=1}^{G^{(h)}}$. The $G^{(h)}$ hypotheses with the highest weights in non-increasing order are obtained by solving the ranked optimal assignment problem [18]. There are many assignment algorithms that solve this optimization problem [31], [32]. Many algorithms are also proposed to solve the ranked assignment problem, where the challenge is to enumerate the N best assignments with lower computational complexity [33]–[35].

Moreover, several processes are applied to tracks and measurements in association matrix S to reduce the number of

Authorized licensed use limited to: GUILIN UNIVERSITY OF ELECTRONIC TECHNOLOGY. Downloaded on June 22,2024 at 10:13:12 UTC from IEEE Xplore. Restrictions apply.

hypotheses, based on the property represented in Remark 2 and the "self-gating" property.

Remark 3: The larger the updated weight $r(z)$ of measurement z, the higher the probability that this measurement is a target.

Thus, based on Remark 2, if $r_U(\Gamma) > T_s, \tau_i \in \Gamma$, the track τ_i is considered to be existing and the corresponding row has $\sum_j S_{i,j} = 1$. Based on Remark 3, if $r(z_j) > \vartheta_z$, where ϑ_z is a preset threshold, this measurement is considered a target and the corresponding column has $\sum_i S_{i,j} = 1$. This means that the significant update components can be known in advance of solving the ranked optimal assignment problem, and many assignments can be excluded, saving substantial computations.

F. Missed Detections

Here, two alternative approaches are proposed to handle the legacy PHD in the τ-LPHD/LCPHD.

1) Alternative 1: The legacy cardinality of the PHD filter is not correctly calculated, while that of the CPHD filter is accurate. For the τ-LPHD, the PHD computed by the δ-GLPHD is used to modify the PHD distribution.

The accurate PHD is given by

$$v(x) = \sum_{(I,\xi)\in\mathcal{F}(\mathbb{L})\times\Xi} v^{(I,\xi)}(x) \tag{74}$$

where

$$v^{(I,\xi)}(x) = \sum_{\ell\in I} w^{(I,\xi)} p^{(\xi)}(x,\ell) \tag{75}$$

is the PHD of hypothesis (I,ξ). This process also can be used for τ-LCPHD, and yields similar results.

2) Alternative 2: Another approach can be used for missed detections in the τ-LCPHD. The weight of the global legacy PHD from the τ-LCPHD is given by

$$r_L = \langle v_L(\cdot), 1\rangle \tag{76}$$

where

$$v_L(x) = \frac{\left\langle \Upsilon_k^1[v_+, Z], \rho_+ \right\rangle}{\left\langle \Upsilon_k^0[v_+, Z], \rho_+ \right\rangle}(1 - p_D(x))v_+(x) \tag{77}$$

Based on the property in Remark 3, the updated weight $r_U(\Gamma)$ of measurement-oriented tracks $\tau \in \Gamma$ is considered proportional to the probability of existence. Thus, the sum of the probabilities of the target disappearing and misdetected can be considered approximate to

$$r_D(\Gamma) + r_L(\Gamma) \approx 1 - r_U(\Gamma) \tag{78}$$

The predicted weight is $r_+(\Gamma)$, and thus the probability of the target disappearing is approximate to $r_D(\Gamma) \approx 1 - r_+(\Gamma)$. Consider constant detection probability p_D: the probability of missed detection is approximate to $r_L(\Gamma) \approx (1 - p_D)r_+(\Gamma)$. The ratio between the disappearing and missed detection can be written as

$$\frac{r_D(\Gamma)}{r_L(\Gamma)} \propto \frac{1 - r_+(\Gamma)}{(1 - p_D)r_+(\Gamma)} \tag{79}$$

Thus the legacy weight is approximate to

$$r_L(\Gamma) \approx \frac{(1 - p_D)r_+(\Gamma)}{1 - p_D r_+(\Gamma)}(1 - r_U(\Gamma)) \tag{80}$$

The legacy PHD is modified by assigning the global legacy weight r_L to those legacy tracks $\tau \in \Gamma$ having $r_L(\Gamma) > 0$. The assignment proportion is calculated by

$$p_L(\tau) = \frac{r_L(\tau)}{\sum_{\Gamma\in\mathbb{T}, r_L(\Gamma)>0} r_L(\Gamma)} \tag{81}$$

The modified legacy PHD is give by

$$v_L^*(x,\tau) \approx p_L(\tau) r_L \cdot \frac{v_+(x,\tau)}{\langle v_+(\cdot,\tau), 1\rangle} \tag{82}$$

3) Comparison of Computational Complexity: If this alternative approach is used for missed detections in τ-LCPHD, the δ-GLCPHD is used only for state estimation and track continuity. While the numerical complexity of the δ-GLPHD is based on the number of propagated hypotheses. If the number of hypotheses is similar to that in the δ-GLMB, the numerical complexity of δ-GLPHD will be similar to that of δ-GLMB. Hence, in the δ-GLCPHD, there is no need to calculate a large number of hypotheses; the K and N of the K-shortest and N-best assignment processes, respectively, a much smaller value compared with the δ-GLPHD, can be taken instead. The disadvantage of the NP-hard problem, that is, the exponential growth in the number of hypotheses, can be greatly alleviated. This approach is applied in this paper, and compared with that in the τ-LPHD.

G. Processes to Improve Performance

The following processes can be used to improve performance.

1) Track Pruning: To reduce the number of tracks, a pruning process is used where the tracks with existence probability below a preset threshold ϑ_p are discarded.

2) Track Merging: There are often a number of PHD components with the same $m(\tau)$. In these cases, the number of components can be reduced, since the tracks are so close together that it is unnecessary to distinguish them by separate PHD components.

If two PHD components $v(x,\tau_i)$ and $v(x,\tau_j)$, with $m(\tau_i) = m(\tau_j)$, have $R_{i,j} = \frac{\langle v(\cdot,\tau_i)\cdot v(\cdot,\tau_j)\rangle}{\langle v(\cdot,\tau_i),1\rangle\langle v(\cdot,\tau_j),1\rangle}$ exceeding a preset threshold ϑ_m, these two PHD components are replaced with $v(x,\tau_l)$, where $v(x,\tau_l) = v(x,\tau_i) + v(x,\tau_j)$ and $\tau_l = \tau_i$ or τ_j. The corresponding mapping σ will also be changed accordingly.

3) Separate Processing for Newborn Targets: To address the issue of response to newborn targets described in subsection III-B, the new tracks are initialized separately. Not only will the transient response to the newborn target be faster and the legacy cardinality estimated more stably, but also the number of subsets generated in the prediction will be significantly reduced.

The adaptive birth intensity for the SMC-CPHD filter proposed in [21] can be applied in the SMC implementation of this work. Also, an efficient adaptive birth model is proposed in [19]. A simple process can be applied when the targets are spontaneously born in a certain region. The scenario is partitioned into a newborn target region and surviving target region, and

Authorized licensed use limited to: GUILIN UNIVERSITY OF ELECTRONIC TECHNOLOGY. Downloaded on June 22,2024 at 10:13:12 UTC from IEEE Xplore. Restrictions apply.

the standard CPHD filter is used for the newborn target region. When newborn targets move out of the birth region, the CPHD of newborn targets and the τ-LCPHD in the survival region are processed together. The cardinality distribution of two CPHDs can be merged as $\rho_M(n) = (\rho_B * \rho_S)(n)$, where $(\rho_B * \rho_S)(n)$ denotes the convolution of $\rho_B(n)$ and $\rho_S(n)$.

H. State Estimation

First, cardinality is estimated based on the cardinality distribution. The cardinality distribution of the τ-LCPHD is obtained, while that of the τ-LPHD can be estimated by

$$\rho(n) = \sum_{L \in \mathcal{F}_n(\mathbb{L})} \sum_{\xi \in \Xi} w^{(\xi)}(L) \tag{83}$$

where $\mathcal{F}_n(\mathbb{L})$ denotes the class of finite subsets of $\mathbb{L}$ with n elements. The cardinality estimate $\hat{N}$ is obtained using a maximum a posteriori (MAP) estimator.

Next, the PHD components and their distinct labels of the best hypothesis with cardinality $\hat{N}$ are chosen for state extraction. Both the MAP and expected a posteriori (EAP) estimates can be obtained with different implementations, e.g., MAP for the GM implementation and EAP for the SMC implementation.

V. Simulations

In this section, a nonlinear multitarget tracking scenario is used to compare the general performance of the proposed LPHD and LCPHD filters with those of the CPHD, CBMeMBer, and LMB filters. Then, a linear scenario is used to compare the performance of tracking accuracy and continuity of the LCPHD filter with the CPHD tracker and LMB filter. The filters here are all implemented with GM implementations.

The GM implementation is based on the standard linear Gaussian assumption [36]. If the dynamic system is nonlinear, the GM implementation can be extended to the extended Kalman filter (EKF), the unscented Kalman filter (UKF) [37], or the cubature Kalman filter (CKF) [38]. Here, the GM implementations in the nonlinear scenario are implemented with the EKF.

A. General Performance

The selected scenario is a simulation of an air surveillance system. The surveillance region is a two-dimensional region $[-50, 50] \times [-50, 50](\text{km})$ with an unknown and time-varying number of targets in the presence of clutter. Target births occur at three specific locations (e.g., airports). In this simulation, there are eight targets in the scenario; the trajectories of these targets are shown in Figure 3.

Each target moves according to the following dynamic model and the target state consists of position and velocity. The state transition model is $x_k = Fx_{k-1} + Gv_k$, where $x_k = [x_{1,k}, x_{2,k}, x_{3,k}, x_{4,k}]^T$ consisting of the position $[x_{1,k}, x_{3,k}]^T$ and velocity $[x_{2,k}, x_{4,k}]^T$, $v = [v_{1,k}, v_{2,k}]^T$ is the process noise

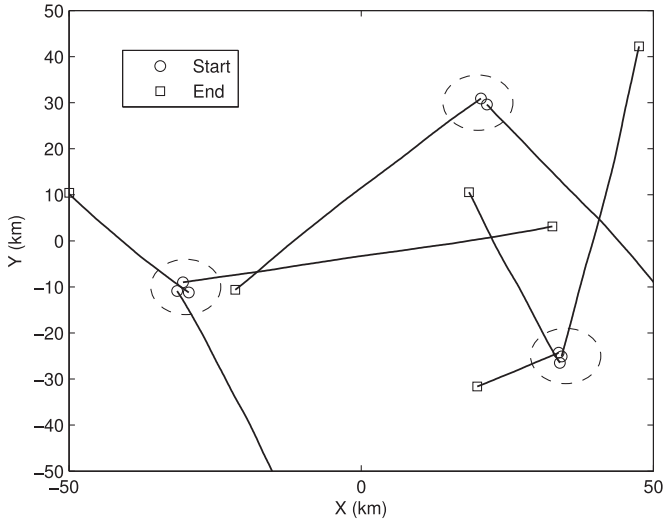

Fig. 3. Trajectories of the eight targets and birth regions (dashed squares).

with standard deviations $\sigma_{v_1} = \sigma_{v_2} = 3\ \text{m}/s^2$, and

$$F = \begin{bmatrix} 1 & T & 0 & 0 \\ 0 & 1 & 0 & 0 \\ 0 & 0 & 1 & T \\ 0 & 0 & 0 & 1 \end{bmatrix}, G = \begin{bmatrix} \frac{T^2}{2} & 0 \\ T & 0 \\ 0 & \frac{T^2}{2} \\ 0 & T \end{bmatrix}$$

The sampling period $T = 1$. New targets are born according to a Poisson RFS with intensity $\gamma_k = \{w_B N_Q(x - \bar{x}_i)\}_{i=1}^3$, where $w_B = 0.01$ and $N_Q(x - \bar{x})$ denotes a normal density with mean $\bar{x}_1 = [-30, 0, -10, 0]^T$, $\bar{x}_2 = [20, 0, 30, 0]^T$, $\bar{x}_3 = [35, 0, -25, 0]^T$ and covariance $Q = \text{diag}([2, 0.2, 2, 0.2]^T)$. The observation model is $z_k = h[x_k, y_k, x_s, y_s] + R_k$, where $R_k = \text{diag}([q_{1,k}, q_{2,k}]^T)$ is mutually independent zero-mean Gaussian white noises with standard deviations $\sigma_{q_1} = (\pi/180)\,\text{rad}$, $\sigma_{q_2} = 20$ m, and

$$h[.] = \begin{bmatrix} \arctan \frac{y_k - y_s}{x_k - x_s} \\ \sqrt{(x_k - x_s)^2 + (y_k - y_s)^2} \end{bmatrix}$$

with sensor position $[x_s, y_s] = [0, -50]^T$km. The detection probability and survival probability are $p_D = 0.97$ and $p_S = 0.99$, respectively. Clutter measurements are uniformly distributed and modeled as a Poisson RFS with mean $r = 10$ per scan over the region $[0, \pi]\,\text{rad} \times [0, 150]\,\text{km}$. The average intensity of clutter is $\lambda_c = 1.06 \times 10^{-2}(\text{rad} \times \text{km})^{-1}$. For the LCPHD filter, the corresponding thresholds are, respectively, $\vartheta_c = 10^{-2}$, $\vartheta_d = 10^{-3}$, $\vartheta_r = 0.9$, $\vartheta_s = 0.9$, and $\vartheta_z = 0.9$.

Pruning and merging are carried out at each time step. For each filter, the pruning threshold is $\vartheta_p = 10^{-5}$ and the merging threshold is $\vartheta_m = 4$. The maximum allowable number of Gaussian components is 100 in the CPHD filter, while it is 20 for each track in the CBMeMBer, LMB, LPHD, and LCPHD filters.

Authorized licensed use limited to: GUILIN UNIVERSITY OF ELECTRONIC TECHNOLOGY. Downloaded on June 22,2024 at 10:13:12 UTC from IEEE Xplore. Restrictions apply.

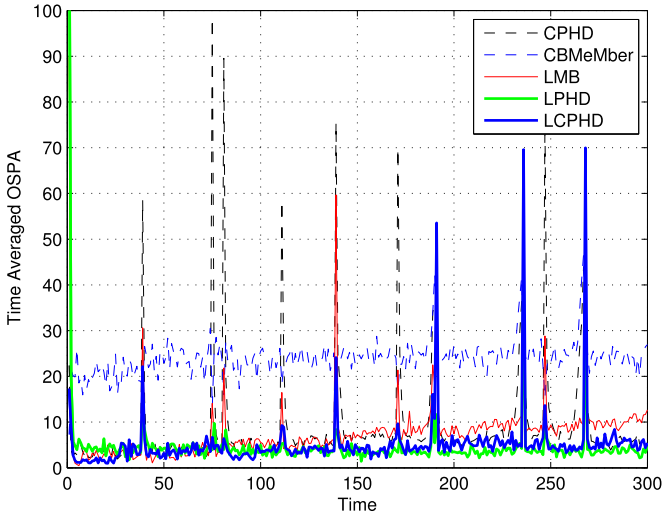

Fig. 4. Mean OSPA distance ($p = 2$ and $c = 200$ km) over 500 Monte Carlo runs.

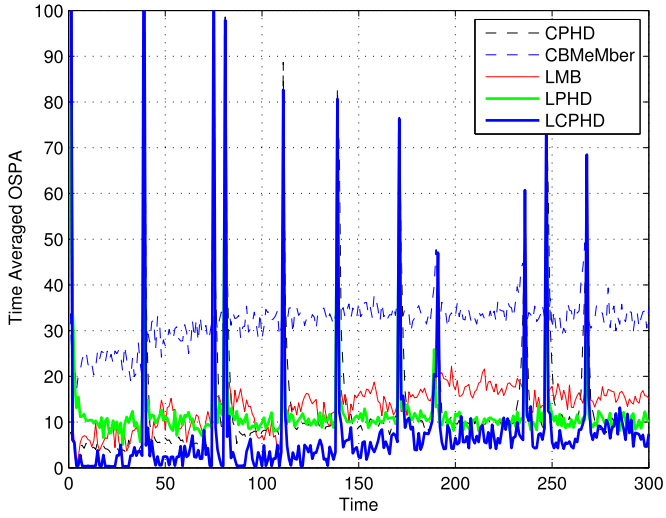

Fig. 6. Mean OSPA distance values over 500 Monte Carlo runs in dense clutter ($r = 70$ per scan).

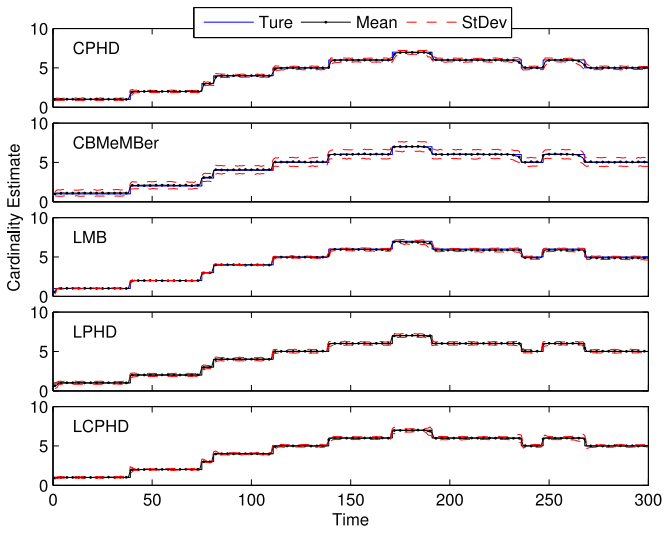

Fig. 5. Mean and standard deviation of cardinality estimates over 500 Monte Carlo runs.

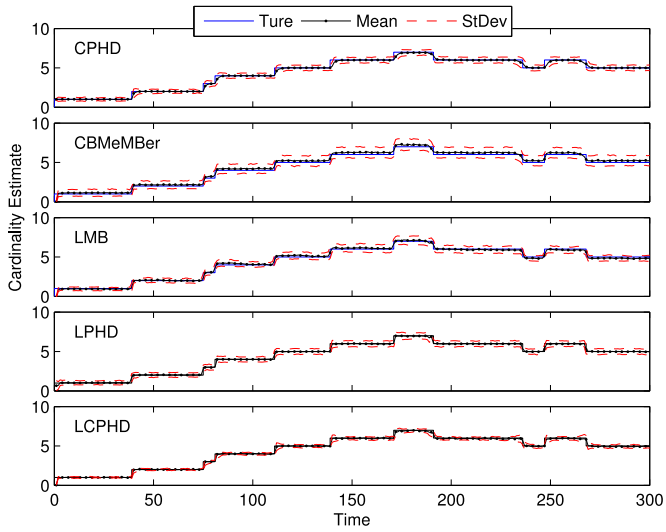

Fig. 7. Mean and standard deviation of cardinality estimates over 500 Monte Carlo runs in dense clutter ($r = 70$ per scan).

1) Monte Carlo Runs: The LPHD and LCPHD filters are compared with the CPHD, CBMeMBer, and LMB filters over 500 Monte Carlo runs. The Optimal Sub-Pattern Assignment (OSPA) miss-distance is used as the metric to evaluate tracking performance [39]. If the scenario is much more complex, the newly proposed Cardinalized Optimal Linear Assignment (COLA) metric [40], which can give better cardinality estimates in some special cases, can be used. The OSPA distance (for $p = 2$ and $c = 200$ km) over 500 Monte Carlo runs is shown in Figure 4. It can be seen that the LPHD and LCPHD filters both perform very well. The means and standard deviations of the cardinality distributions over 500 Monte Carlo runs are shown in Figure 5. The CPHD, LMB, LPHD, and LCPHD filters all have low variance on estimated cardinality. Compared with the CPHD filter, the better performance of the LCPHD filter when new targets appear certifies the response of the CPHD filter to newborn targets. The CBMeMBer filter has the worst performance of the five filters evaluated. The LMB filter performs slightly better than the CPHD filter before 150 time steps, but worse when targets are separating after intersection. Since there is an LMB approximation to the multitarget posterior, the distributions of tracks with the same label may be merged in the filtering. If the targets are closely-spaced, the distribution of a track (label) may be ambiguous.

2) Dense Clutter Scenario: Given dense clutter rates of $r = 70$ per scan, Figure 6 and Figure 7 show the average OSPA distances and the means and standard deviations of the cardinality distributions over 500 Monte Carlo runs, respectively. It can be seen that the LCPHD filter performs significantly better than the other filters, because of the stable modified cardinality estimated by the LCPHD filter. Moreover, the CBMeMBer filter has a positive bias in cardinality estimates.

3) Low Detection Probability Scenario: The detection probability is decreased to $p_D = 0.7$. In Figure 8 and Figure 9, the

Authorized licensed use limited to: GUILIN UNIVERSITY OF ELECTRONIC TECHNOLOGY. Downloaded on June 22,2024 at 10:13:12 UTC from IEEE Xplore. Restrictions apply.

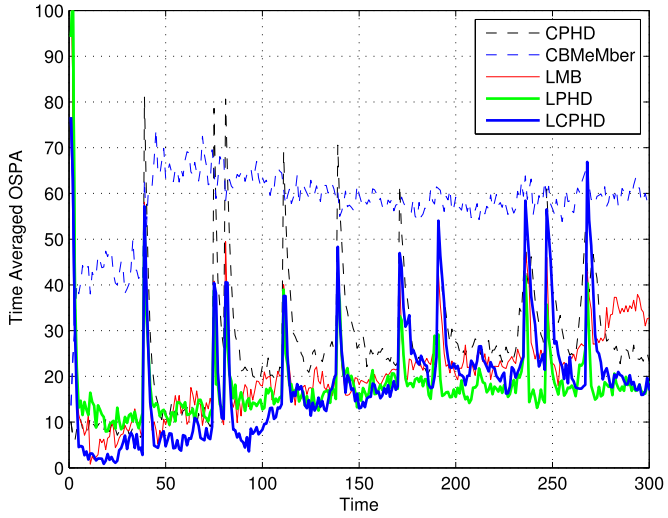

Fig. 8. Mean OSPA distance values over 500 Monte Carlo runs in low detection probability ($p_D = 0.7$).

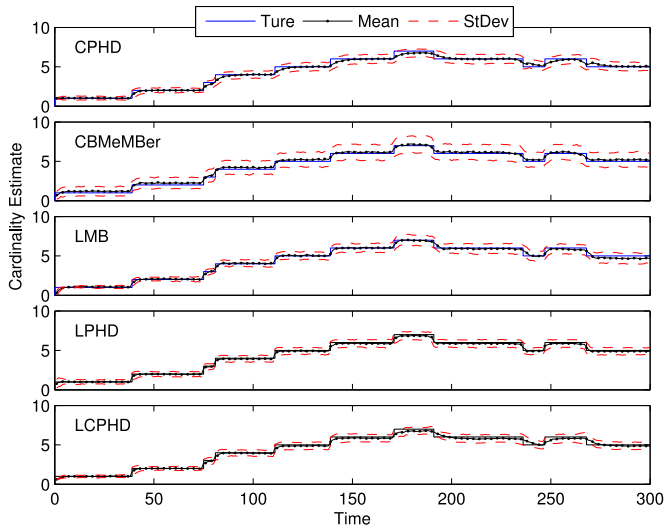

Fig. 9. Mean and standard deviation of cardinality estimates over 500 Monte Carlo runs in low detection probability ($p_D = 0.7$).

average OSPA distances and the means and standard deviations of the cardinality distributions over 500 Monte Carlo runs are shown, respectively. The LMB, LPHD, and LCPHD filters perform well, with stable cardinality estimates, while the CBMeMBer filter performs poorly, with much higher variances on estimated cardinality. The CBMeMBer filter also has a positive bias in cardinality estimates.

4) Computational Load: The averaged OSPA distances over 300 scans and the mean CPU times over 500 Monte Carlo runs are shown in Table II. The code is written in MATLAB and run on Intel i7 4-Core 3.5GHz CPU, which can be further improved with an optimized C++ implementation. It can be seen that the LCPHD filter has a lower computational load than the LPHD filter, due to the small number of hypotheses. But, at times, the LPHD may perform better than LCPHD because the larger number of hypotheses in LPHD may contain more accurate information.

TABLE II
AVERAGED OSPA DISTANCE OVER 300 SCANS AND MEAN CPU TIME IN 500 MONTE CARLO RUNS

Filter	OSPA (km)	OSPA (km) ($r = 70$)	OSPA (km) ($p_D = 0.7$)	CPU time (s)		
CPHD	9.0055	13.1076	25.9976	6.8	35.5	7.3
CBMeMBer	23.9385	32.7066	57.8610	14.8	40.2	38.4
LMB	7.9077	14.5862	21.4282	33.9	49.2	35.9
LPHD	4.7514	12.1266	17.8451	14.8	54.2	37.6
LCPHD	5.1142	8.3120	18.3763	8.1	43.8	25.6

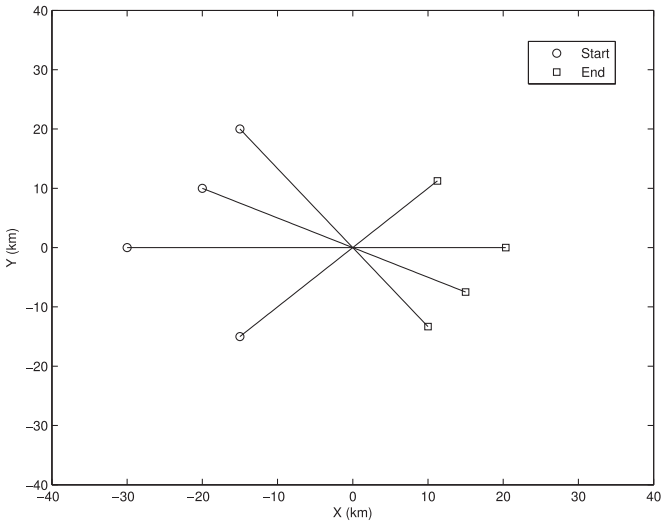

Fig. 10. Trajectories of the four crossing targets.

B. Tracking Accuracy and Continuity

Two scenarios consisting of four crossing targets are used to demonstrate the tracking accuracy and continuity of the proposed filter. The performance of the LCPHD filter, which considers only a small number of hypotheses, is evaluated here. The first scenario is shown in Figure 10.

The target state consists of position and velocity and the dynamic model is the same as that in the previous simulation. The process noise has standard deviations of $\sigma_{v_1} = \sigma_{v_2} = 10\mathrm{m}/s^2$. The observation model is $z_k = Hx_k + R_k$, where $H = [T, 0, 0, 0; 0, 0, T, 0]$ and $R_k = \mathrm{diag}([q_{1,k}, q_{2,k}]^T)$ with $\sigma_{q_1} = \sigma_{q_2} = 30$ m. The detection probability and survival probability are $p_D = 0.99$ and $p_S = 0.99$, respectively. Clutter is uniformly distributed and modeled as a Poisson RFS with mean $r = 10$ per scan over the observation region.

An estimate-to-track association method is proposed in [41]. This algorithm is based on a tree-structured track management scheme for the GM-PHD filter, and can be applied to the GM-CPHD filter as well. However, this algorithm only considers the score of track hypotheses in each tree by summing log likelihood ratios (LLR), and does not consider the relationships between trees. The confusion occurs when Gaussian components with different labels are merged into one. Furthermore, more than one tree may consider the same track as the correct association track hypothesis.

The OSPA-T metric is proposed in [42] to capture the difference between the two sets of tracks in the cardinality error, localization error, and labeling error. The parameters of the

Authorized licensed use limited to: GUILIN UNIVERSITY OF ELECTRONIC TECHNOLOGY. Downloaded on June 22,2024 at 10:13:12 UTC from IEEE Xplore. Restrictions apply.

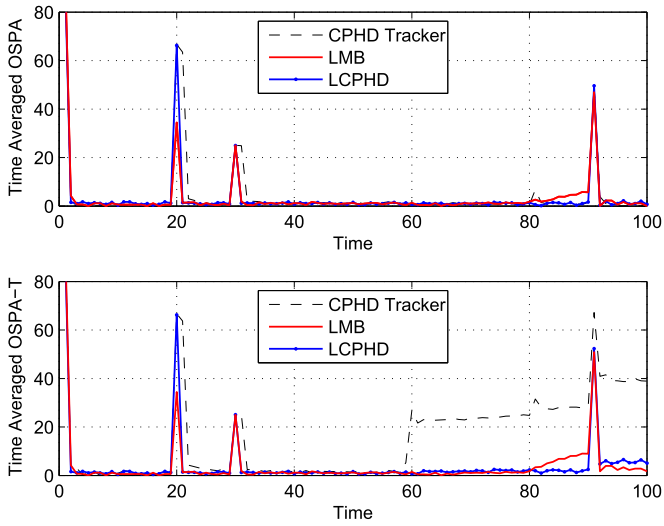

Fig. 11. OSPA distance and OSPA-T distance over 300 Monte Carlo runs.

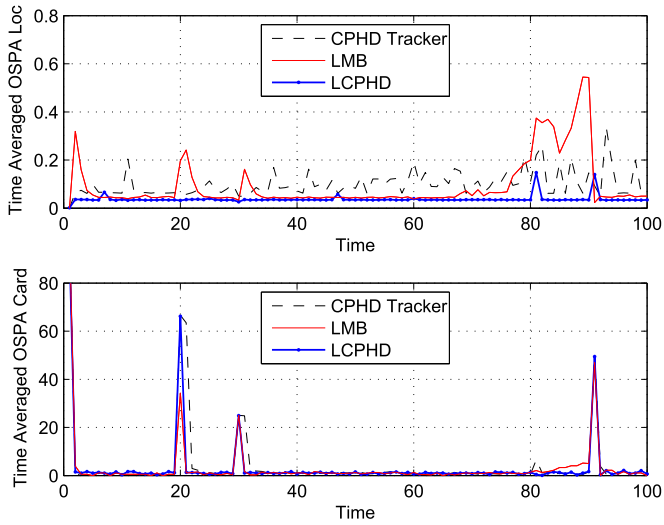

Fig. 12. OSPA components over 300 Monte Carlo runs.

OSPA-T metric used in evaluation are $p = p' = 1$, $c = 100$ m, and $\alpha = 100$. Figure 11 shows the OSPA distance and the OSPA-T distance. It can be seen that the labeling error of the CPHD tracker is much larger than for the LMB and LCPHD filters.

Since the LCPHD filter uses the PHD components associated with the corresponding track and measurement for state extraction in the δ-GLCPHD filtering recursion, the state estimation is not affected by the minor modes from the incorrect association. Figure 12 shows the OSPA localization and cardinality components. The LMB and LCPHD filters have better localization performance than the CPHD tracker due to the more accurate propagation of the posterior density. The performance of LMB degrades when the four targets separate after the intersection point, because that tracks with same label and similar weight may be merged and the distribution of a label becomes ambiguous.

The second scenario narrows the crossing angle and makes it harder to maintain track continuity, as shown in Figure 13. Figure 14 shows the OSPA distance and the OSPA-T distance. The LMB and LCPHD filters significantly outperform the CPHD

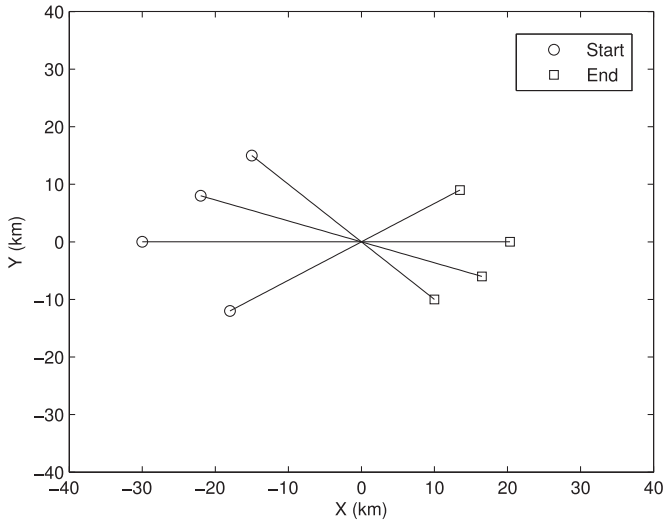

Fig. 13. Trajectories of the four crossing targets.

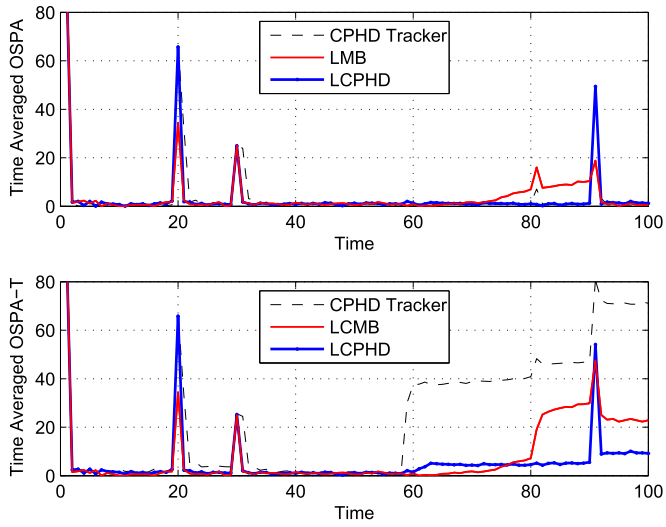

Fig. 14. OSPA distance and OSPA-T distance over 300 Monte Carlo runs.

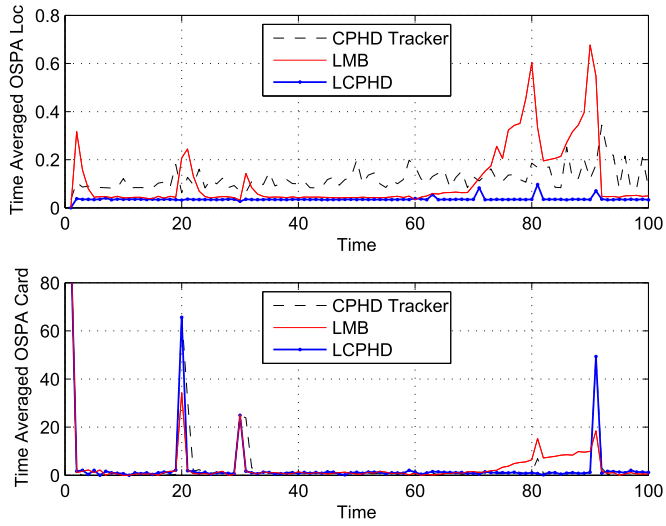

Fig. 15. OSPA components over 300 Monte Carlo runs.

Authorized licensed use limited to: GUILIN UNIVERSITY OF ELECTRONIC TECHNOLOGY. Downloaded on June 22,2024 at 10:13:12 UTC from IEEE Xplore. Restrictions apply.

tracker in maintaining track continuity. Moreover, the LMB and LCPHD filters have better localization performances, as shown in Figure 15.

VI. Conclusions

In this paper, two new labeled multitarget Bayes filters were proposed. The proposed LPHD filter uses the τ-LPHD as a "PHD look-ahead" strategy and saves substantial computational resources in the δ-GLPHD, which is similar to the δ-GLMB, but uses the information from the τ-LPHD to improve on computational efficiency. This look-ahead approach indicates which hypotheses need not be considered and how many hypotheses need be propagated. While the δ-GLCPHD in the proposed LCPHD filter is used only for state estimation and track continuity, the consequence is that a much smaller number of hypotheses are needed, and thus the computational load of the LCPHD filter is significantly lower than for other filters. In the τ-LCPHD, a stable cardinality estimate was obtained, since the legacy PHD of missed detections was distributed to corresponding tracks. Simulations show that the LPHD and LCPHD filters outperform the CPHD, CBMeMBer, and LMB filters. Furthermore, compared with the CPHD tracker and LMB filter, the LCPHD filter was shown to have the capability of maintaining stable track continuity and achieving accurate localization performance.

Appendix A
Pseudo-code for the LPHD/LCPHD filters

Step 1. Prediction of the τ-LPHD/LCPHD
input: v and v_B
compute $v_{+,S}$ using (34)
compute ρ_+ using (36) (τ-LCPHD)
output: v_+ and ρ_+

Step 2. Update of the τ-LPHD/LCPHD
input: v_+, ρ_+ and Z
compute v' using (41)
compute v using (42) (τ-LPHD)
compute v using (45) (τ-LCPHD)
compute ρ using (46) (τ-LCPHD)
output: v', v and ρ

Step 3. Pre-processing
input: v
compute W using (53)
compute $r(z)$ using (54)
compute $r_U(\Gamma)$ using (55)
$\Omega \leftarrow W$
use function β to partition Ω into $\{\Omega_n\}_{n=1}^{N}$
output: $r(z)$, $r_U(\Gamma)$ and $\{\Omega_n\}_{n=1}^{N}$

Step 4. Prediction of the δ-GLPHD/GLCPHD
input: $\{(I^{(h)}, \sigma^{(h)}, \xi^{(h)}, w^{(h)}, v^{(h)}, K^{(h)})\}_{h=1}^{H}$, $\{(r_B^{(\ell)}, v_B^{(\ell)})\}_{\ell\in\mathbb{B}}$ and v_+
$\{L^{(b)}\}_{b=1}^{K_B} \leftarrow (\mathbb{B}, K_B)$, determine $K_B = 2^{n_B}$ based on updated PHD; use K-shortest paths if K_B is still large
for $b = 1 : K_B$
  compute $w_B^{(b)}$ using (60)
end
for $h = 1 : H$
  $\{J^{(h,j)}\}_{j=1}^{K^{(h)}} \leftarrow (I^{(h)}, K^{(h)})$, determine $K^{(h)} = 1^{n_1} 2^{n_2}$ based on updated PHD; use K-shortest paths if $K^{(h)}$ is still large
  for $(j, b) = (1, 1) : (K^{(h)}, K_B)$
    $I_+^{(h,j,b)} \leftarrow J^{(h,j)} \cup L^{(b)}$
    $\sigma_+^{(h,j,b)} \leftarrow \sigma^{(h,j)} \cup \sigma^{(b)}$
    compute $w_+^{(h,j,b)}$ using (61), based on v_+ from Step 1
  end
end
normalize weights $\{w_+^{(h,j,b)}\}_{(h,j,b)=(1,1,1)}^{(H,K^{(h)},K_B)}$ (δ-GLPHD)
output: $\{(I_+^{(h,j,b)}, \sigma_+^{(h,j,b)}, w_+^{(h,j,b)}, v_+^{(h,j,b)})\}_{(h,j,b)=(1,1,1)}^{(H,K^{(h)},K_B)}$

Step 5. Update of the δ-GLPHD/GLCPHD
input: $\{(I^{(h)}, \sigma^{(h)}, \xi^{(h)}, w^{(h)}, v^{(h)}, M^{(h)})\}_{h=1}^{H}$, v', $r(z)$, $r_U(\Gamma)$, $\{\Omega_n\}_{n=1}^{N}$ and Z
for $h = 1 : H$
  for $n = 1 : N$
    compute $C^{(h,n)}$ using (71)
    use $r(z)$ and $r_U(\Gamma)$ from Step 3 to reduce the number of the association maps θ in group Ω_n
    $\{\theta^{(h,n,j)}\}_{j=1}^{G^{(h,n)}} \leftarrow (I^{(h,n)}, C^{(h,n)}, T^{(h,n)})$, compute $G^{(h,n)}$ for group Ω_n and use assignment algorithm if $G^{(h,n)}$ is still large
  end
  $G^{(h)} \leftarrow \{G^{(h,n)}\}_{n=1}^{N}$
  for $j = 1 : G^{(h)}$
    compute $w^{(h,j)}$ using (66), based on v' from Step 2
    $I^{(h,j)} \leftarrow I^{(h)}$
    $\xi^{(h,j)} \leftarrow (\xi^{(h)}, \theta^{(h,j)})$
  end
end
normalize weights $\{w^{(h,j)}\}_{(h,j)=(1,1)}^{(H,T^{(h)})}$ (δ-GLPHD)
output: $\{(I^{(h,j)}, \sigma^{(h,j)}, \xi^{(h,j)}, w^{(h,j)}, v^{(h,j)})\}_{(h,j)=(1,1)}^{(H,G^{(h)})}$

Step 6. Legacy PHD modification of τ-LPHD/LCPHD
input: v (τ-LPHD) or v_L (τ-LCPHD)
modify v using (74) (τ-LPHD)
modify legacy PHD v_L using (82) (τ-LCPHD)
output: v (τ-LPHD) or v_L (τ-LCPHD)

References

[1] Y. Bar-Shalom, P. K. Willett, and X. Tian, *Tracking and Data Fusion*. New York, NY, USA: YBS Publishing, 2011.
[2] S. S. Blackman, *Multiple Target Tracking with Radar Applications*. Norwood, MA, USA: Artech House, 2001.
[3] R. Mahler, *Statistical Multisource-Multitarget Information Fusion*. Norwood, MA, USA: Artech House, 2007.
[4] Y. Bar-Shalom, X. R. Li, and T. Kirubarajan, *Estimation With Applications to Tracking and Navigation*. New York, NY, USA: Wiley, 2001.

Authorized licensed use limited to: GUILIN UNIVERSITY OF ELECTRONIC TECHNOLOGY. Downloaded on June 22,2024 at 10:13:12 UTC from IEEE Xplore. Restrictions apply.

[5] S. Blackman, "Multiple hypothesis tracking for multiple target tracking," *IEEE Aerosp. Electron. Syst. Mag.*, vol. 19, no. 1, pp. 5–18, Jan. 2004.
[6] T. Fortmann, Y. Bar-Shalom, and M. Scheffe, "Sonar tracking of multiple targets using joint probabilistic data association," *IEEE J. Ocean. Eng.*, vol. 8, no. 3, pp. 173–184, Jul. 1983.
[7] L. Lin, Y. Bar-Shalom, and T. Kirubarajan, "Data association combined with the probability hypothesis density filter for multitarget tracking," *Proc. SPIE*, vol. 5428, pp. 464–475, 2004.
[8] R. Mahler, "Multitarget Bayes filtering via first-order multitarget moments," *IEEE Trans. Aerosp. Electron. Syst.*, vol. 39, no. 4, pp. 1152–1178, Oct. 2003.
[9] R. Mahler, "PHD filters of higher order in target number," *IEEE Trans. Aerosp. Electron. Syst.*, vol. 43, no. 4, pp. 1523–1543, Oct. 2007.
[10] B.-T. Vo, B.-N. Vo, and A. Cantoni, "The cardinality balanced multi-target multi-Bernoulli filter and its implementations," *IEEE Trans. Signal Process.*, vol. 57, no. 2, pp. 409–423, Feb. 2009.
[11] D. Clark and J. Bell, "Multi-target state estimation and track continuity for the particle PHD filter," *IEEE Trans. Aerosp. Electron. Syst.*, vol. 43, no. 4, pp. 1441–1453, Oct. 2007.
[12] D. Clark, K. Panta, and B.-N. Vo, "The GM-PHD filter multiple target tracker," in *Proc. 9th Int. Conf. Inf. Fusion*, Jul. 2006, pp. 1–8.
[13] K. Panta, D. Clark, and B.-N. Vo, "Data association and track management for the Gaussian mixture probability hypothesis density filter," *IEEE Trans. Aerosp. Electron. Syst.*, vol. 45, no. 3, pp. 1003–1016, Jul. 2009.
[14] L. Lin, Y. Bar-Shalom, and T. Kirubarajan, "Track labeling and PHD filter for multitarget tracking," *IEEE Trans. Aerosp. Electron. Syst.*, vol. 42, no. 3, pp. 778–795, Jul. 2006.
[15] K. Panta, B.-N. Vo, and S. Singh, "Novel data association schemes for the probability hypothesis density filter," *IEEE Trans. Aerosp. Electron. Syst.*, vol. 43, no. 2, pp. 556–570, Apr. 2007.
[16] E. Pollard, B. Pannetier, and M. Rombaut, "Hybrid algorithms for multitarget tracking using MHT and GM-CPHD," *IEEE Trans. Aerosp. Electron. Syst.*, vol. 47, no. 2, pp. 832–847, Apr. 2011.
[17] B-T. Vo and B-N. Vo, "Labeled random finite sets and multi-object conjugate priors," *IEEE Trans. Signal Process.*, vol. 61, no. 13, pp. 3460–3475, Jul. 2013.
[18] B-N. Vo, B-T. Vo, and D. Phung, "Labeled random finite sets and the Bayes multi-target tracking filter," *IEEE Trans. Signal Process.*, vol. 62, no. 24, pp. 6554–6567, Dec. 2014.
[19] S. Reuter, B-T. Vo, B-N. Vo, and K. Dietmayer, "The labeled multi-Bernoulli filter," *IEEE Trans. Signal Process.*, vol. 62, no. 12, pp. 3246–3260, Jun. 2014.
[20] B-T. Vo, B-N. Vo, and A. Cantoni, "Analytic implementations of the cardinalized probability hypothesis density filter," *IEEE Trans. Signal Process.*, vol. 55, no. 7, pp. 3553–3567, Jul. 2007.
[21] B. Ristic, D. Clark, B-N. Vo, and B-T. Vo, "Adaptive target birth intensity for PHD and CPHD filters," *IEEE Trans. Aerosp. Electron. Syst.*, vol. 48, no. 2, pp. 1656–1668, Apr. 2012.
[22] R. Mahler, B-T. Vo, and B-N. Vo, "CPHD filtering with unknown clutter rate and detection profile," *IEEE Trans. Signal Process.*, vol. 59, no. 8, pp. 3497–3513, Aug. 2011.
[23] R. Georgescu and P. Willett, "The multiple model CPHD tracker," *IEEE Trans. Signal Process.*, vol. 60, no. 4, pp. 1741–1751, Apr. 2012.
[24] M. Lundgren, L. Svensson, and L. Hammarstrand, "A CPHD filter for tracking with spawning models," *IEEE J. Sel. Topics Signal Process.*, vol. 7, no. 3, pp. 496–507, Jun. 2013.
[25] D. Fränken, M. Schmidt, and M. Ulmke, "'Spooky action at a distance' in the cardinalized probability hypothesis density filter," *IEEE Trans. Aerosp. Electron. Syst.*, vol. 45, no. 4, pp. 1657–1664, Oct. 2009.
[26] R. Mahler, *Advances in Statistical Multisource-Multitarget Information Fusion*. Norwood, MA, USA: Artech House, 2014.
[27] B. N. Vo, B. T. Vo, and H. Hoang, "An efficient implementation of the generalized labeled multi-bernoulli filter," *IEEE Trans. Signal Process.*, vol. 65, no. 8, pp. 1975–1987, Apr. 2017.
[28] O. Erdinc, P. Willett, and Y. Bar-Shalom , "The bin-occupancy filter and its connection to the PHD filters," *IEEE Trans. Signal Process.*, vol. 57, no. 11, pp. 4232–4246, Nov. 2009.
[29] D. Dunne and T. Kirubajaran, "Weight partitioned probability hypothesis density filters," in *Proc. 14th Int. Conf. Inf. Fusion*, Jul. 2011, pp. 1826–1833.
[30] D. Eppstein, "Finding the k shortest paths," *SIAM J. Comput.*, vol. 28, no. 2, pp. 652–673, 1999.
[31] H. W. Kuhn, "The Hungarian method for the assignment problem," *Naval Res. Logist.*, vol. 2, no. 1/2, pp. 83–97, 1955.
[32] M. Balinski and R. Gomory, "A primal method for the assignment and transportation problems," *Manage. Sci.*, vol. 10, no. 3, pp. 578–593, 1964.
[33] K. Murthy, "An algorithm for ranking all the assignments in order of increasing costs," *Oper. Res.*, vol. 16, no. 3, pp. 682–687, 1968.
[34] M. Miller, H. Stone, and I. J. Cox, "Optimizing Murty's ranked assignment method," *IEEE Trans. Aerosp. Electron. Syst.*, vol. 33, no. 3, pp. 851–862, Jul. 1997.
[35] I. Cox and M. Miller, "On finding ranked assignments with application to multitarget tracking and motion correspondence," *IEEE Trans. Aerosp. Electron. Syst.*, vol. 31, no. 1, pp. 486–489, Jan. 1995.
[36] H. W. Sorenson and D. L. Alspach, "Recursive Bayesian estimation using Gaussian sums," *Automatica*, vol. 7, no. 4, pp. 465–479, 1971.
[37] B.-N. Vo and W.-K. Ma, "The Gaussian mixture probability hypothesis density filter," *IEEE Trans. Signal Process.*, vol. 54, no. 11, pp. 4091–4104, Nov. 2006.
[38] I. Arasaratnam and S. Haykin, "Cubature Kalman filters," *IEEE Trans. Autom. Control*, vol. 54, no. 6, pp. 1254–1269, Jun. 2009.
[39] D. Schuhmacher, B-T. Vo, and B-N. Vo, "A consistent metric for performance evaluation of multi-object filters," *IEEE Trans. Signal Process.*, vol. 56, no. 8, pp. 3447–3457, Aug. 2008.
[40] P. Barrios, G. Naqvi, M. Adams, K. Leung, and F. Inostroza, "The cardinalized optimal linear assignment (COLA) metric for multi-object error evaluation," in *Proc. 18th Int. Conf. Inf. Fusion*, Jul. 2015, pp. 271–279.
[41] K. Panta, D. Clark, and B-N. Vo, "Data association and track management for the gaussian mixture probability hypothesis density filter," *IEEE Trans. Aerosp. Electron. Syst.*, vol. 45, no. 3, pp. 1003–1016, Jul. 2009.
[42] B. Ristic, B-N. Vo, D. Clark, and B-T. Vo, "A metric for performance evaluation of multi-target tracking algorithms," *IEEE Trans. Signal Process.*, vol. 59, no. 7, pp. 3452–3457, Jul. 2011.

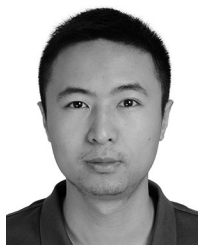

Zhejun Lu was born in March 1989. He received the B.S. and M.S. degrees in information and communication engineering from the National University of Defense Technology, Changsha, China, in 2011 and 2013, respectively, where he is currently working toward the Ph.D. degree. From September 2014 to September 2015, he was studying in McMaster University, Hamilton, ON, Canada as a visiting Ph.D. student.

His research interests include estimation, signal processing, and tracking.

Weidong Hu was born in September 1967. He received the B.S. degree in microwave technology and the M.S. and Ph.D. degrees in communication and electronic system from the National University of Defense Technology, Changsha, China, in 1990, 1994, and 1997, respectively.

He is currently a Full Professor in the ATR Laboratory, National University of Defense Technology, Changsha. His research interests include radar signal and data processing.

Thiagalingam Kirubarajan (S'95–M'98–SM'03) received the B.A. and M.A. degrees in electrical and information engineering from Cambridge University, Cambridge, U.K., in 1991 and 1993, and the M.S. and Ph.D. degrees in electrical engineering from the University of Connecticut, Storrs, CT, USA. He holds the title of Distinguished Engineering Professor and holds the Canada Research Chair in Information Fusion at McMaster University, Hamilton, ON, Canada. He has published about 350 research articles, 11 book chapters, one standard textbook on target tracking and four edited volumes. He has led multiple projects on tracking and fusion with support from the Canadian Department of National Defense, US Air Force, US Navy, NASA, NSERC, Ontario Ministry of Research and Innovation, General Dynamics Canada, Raytheon Canada, ComDev/exactEarth, Toyota, Mine Radio Systems, Qualtech, FLIR Radar Systems, and Lockheed Martin Canada. As part of his research at McMaster University, he led the design and development of the distributed multisensor-multitarget tracking testbed for scenario generation, tracking algorithm development, and performance evaluation. He has received Ontario Premier's Research Excellence Award and IEEE AESS Barry Carlton Award.

Authorized licensed use limited to: GUILIN UNIVERSITY OF ELECTRONIC TECHNOLOGY. Downloaded on June 22,2024 at 10:13:12 UTC from IEEE Xplore. Restrictions apply.